DRAL
Daresbury Laboratory
Rutherford Appleton Laboratory

RAL Report
RAL-95-007

A Method of Estimating the Response Functions of a Multi-Input Linear System

T Dewson and AD Irving

January 1995

Rutherford Appleton Laboratory Chilton DIDCOT Oxfordshire OX11 0QX

A METHOD OF ESTIMATING THE RESPONSE FUNCTIONS OF A MULTI-INPUT LINEAR SYSTEM

T Dewson
Department of Mathematics,
University of Bristol,
University Walk,
Bristol, BS8 1TW, UK.

AD Irving
Nonlinear Time Series Group,
Rutherford Appleton Laboratory,
Chilton, Didcot,
Oxon, OX11 0QX, UK.

Abstract

In this work a novel formalism to estimate the vector linear impulse response functions from the experimental data observed from a multi-input system, allowing for correlation between the inputs, is developed. Time series statistical moments are estimated from the data and used as the basis of a set of simultaneous equations in the unknown response functions. These simultaneous equations are solved using standard matrix methods for the unknown linear response functions. This approach is an extension to one proposed by Box and Jenkins from the Yule-Walker equations. The ability of the technique to correctly estimate the response functions of a multi-input linear system to a high degree of accuracy is demonstrated, using a numerical example where the properties of the system are known and there is strong correlation between the input data. This novel technique is then used to estimate the response functions of the coupled convective and radiative processes, that act at the internal surface of the ceiling of an experimental building. The area under the estimated response function of each process is the gain or heat transfer coefficient for that process. The estimated response functions from a multi-input analysis are compared with those obtained from a set of analyses where each input is treated as being independant of the others. The response functions, of each process, estimated by the two approaches (single- and multi- input) were employed to predict an out of sample period of the surface heat flux, given the convective and radiative driving forces, which could be compared with the measured heat flux. The differences between the results obtained from the two approaches are explained by considering the correlation between the driving forces of the convective and radiative processes.

Introduction

The analysis of time series data from dynamical systems is an important issue in numerous areas of science and engineering, and the study of linear systems has dominated scientific thinking for many years. A linear system has the property that the output produced is proportional to the input and that any complexity that arises may be described as the result of superposition. The useful property of linear superposition implies that the output from a linear system is the summation, over all inputs, of the response of that system to each input, as if it were the only input to the system. However in reality most, if not all, physical systems exhibit non-linear behaviour to some extent, and this makes them difficult to study . But fortunately many systems can be assumed to behave in an approximately linear manner in a limited region of operation. However there are few analysis techniques availible to the experimentalist that can extract the relevant information, about even a linear system, from the time series data.

The most common tools employed for the analysis of time series data from linear systems are the linear correlation function and it's Fourier transform, the spectral density. These tools are, respectively, applied in the least squares maximum likelihood estimation of a set parameters for an auto-regressive moving-average model, commonly known as the Box and Jenkins approach [1], and in the response function estimation technique in the frequency domain (for example, [2]). For both these approaches, a technique for the estimation of the response functions of a multi-input system has been developed ([1], and for example, [2]).

Recently a generalised theory for the estimation of the impulse response functions of single-input mixed order (linear + non-linear) system has been developed [3]. This technique is based on the Volterra series, which is the generalisation of the linear convolution equation, and employs the statistical time delayed moments of the input and output time series in a characterisation of the system in terms of it's impulse response functions. The impulse response function is a widely used means for the characterisation of a system (for example, [4]). In that work, an absolute time frame of reference for the time delayed moments, rather than the standard, more commonly used retarded time frame, was employed. This difference, i.e the use of the absolute time frame, was shown to be important, and hence will be continued to be used in this work.

In this paper, a new technique for the estimation of the linear response functions of a multi-input system is presented, which uses the same analysis formalism as developed in the non-linear analysis technique. That is, the use of the time delayed statistical moments between the input and output data. The single-input linear case of the non-linear technique has recently been applied to the estimation of the surface heat transfer coefficient of the ceiling in an experimental building [5]. In that application, the air-surface temperature difference and the heat flux at the surface of the ceiling were, respectively, the single input to and single output from the model. The single-input linear technique was employed to estimate the response function for the convective process occuring at the ceiling. The multi-input technique, developed in this work, will be applied to a full linear analysis of this surface heat flux data, accounting for all the factors that affect the heat flux at the surface, i.e the convective, radiative and conductive processes, and the results obtained compared with those obtained from single-input analyses.

Estimation of the linear response functions of a multi-input system

In this section, a novel analysis technique for the estimation of the impulse response functions of a multi-input linear system, allowing for correlation between the inputs to the system, is presented. The response functions are used to characterise the properties of the system, in terms of it's physical observables. From this characterisation, inferences may be made about the properties of the system, in terms of physical laws, formulae, the form of the basis set, or the like. This characterisation, or identification of a model, of the physical system, given observations of the input and output time series data of the system, is thus an important problem in numerous areas of science. The single-input single-output linear convolution equation, and it's equivalent in the frequency domain, is the most important input-output relationship for a linear system (for example, [2, 4]).

$$y(t) = \sum_{\tau=0}^{\mu} h_{yx}(\tau) x(t-\tau)$$

It conveys that the output of the system at the present time, t, $y(t)$, is dependant upon the current (time, t) and previous (time, $t-\tau$) values of the input, $x(t-\tau)$, through a weighting

or linear response function, $h_{yx}(\tau)$. That is the output has some 'memory' of length μ, of the previous values of the input time series. This equation can be easily extended to the multi-input case (for example, [1, 2, 4])

Consider a system with N inputs and one output, from which the observed time series data is given by $x_i(t), i = 1, \ldots, N$ for the inputs, and $y(t)$ for the output. It is usual to draw on a number of assumptions, in developing a model of this system, when analysing the observed data. These are that the system is linear, causal, time-invariant, has a finite length memory, and that the boundary conditions $x_i(t), i = 1, \ldots, N$ and $y(t)$ are drawn from stationary stochastic sequences for which the second order time series moments exist.

$$y(t) = \sum_{\tau=0}^{\mu} h_{yx_1}(\tau)x_1(t-\tau) + \ldots\ldots + \sum_{\tau=0}^{\mu} h_{yx_i}(\tau)x_i(t-\tau) + \ldots\ldots + \sum_{\tau=0}^{\mu} h_{yx_N}(\tau)x_N(t-\tau)$$

which can be written in the following shortened form,

$$y(t) = \sum_{i=1}^{N}\sum_{\tau=0}^{\mu} h_{yx_i}(\tau)x_i(t-\tau) \tag{1}$$

where $h_{yx_i}(\tau)$ represents the linear response function of the output to the ith input channel. However this simple extention belies the difficulty associated with the estimation of these response functions. Currently there exist least squares parameter estimation techniques (for example, [1]) and a frequency domain techniques (for example, [2]), however there is no complementary working technique in the time delay domain, this new technique overcomes this deficiency.

As the boundary conditions are assumed to be drawn from stationary stochastic sequences, it is thus possible to use time series moments to characterise the response of the system, as an alternative to the multi-input convolution equation, given in equation (1). The authors have recently developed a formalism for the estimation of the linear and non-linear response functions of a mixed order system, involving the formation and solution of a set of simultaneous equations relating the time delayed moments between the input and output time series data [5]. This formalism is adopted in this work, and used to developed a set of simultaneous equations, from which the unknown response functions can be calculated.

The first equation in this set of simultaneous equations is formed by multiplying equation (1) by $x_1(t-k)$, where k denotes an arbitrary time delay, to give

$$\begin{aligned} x_1(t-k)y(t) &= \sum_{\tau=0}^{\mu} h_{yx_1}(\tau)x_1(t-k)x_1(t-\tau) + \sum_{\tau=0}^{\mu} h_{yx_2}(\tau)x_1(t-k)x_2(t-\tau) \\ &\quad + \ldots\ldots + \sum_{\tau=0}^{\mu} h_{yx_i}(\tau)x_1(t-k)x_i(t-\tau) \\ &\quad + \ldots\ldots + \sum_{\tau=0}^{\mu} h_{yx_N}(\tau)x_1(t-k)x_N(t-\tau) \end{aligned}$$

By applying the expectation operator to this this equation, we obtain

$$\begin{aligned} E[x_1(t-k)y(t)] &= \sum_{\tau=0}^{\mu} h_{yx_1}(\tau)E[x_1(t-k)x_1(t-\tau)] + \sum_{\tau=0}^{\mu} h_{yx_2}(\tau)E[x_1(t-k)x_2(t-\tau)] \\ &\quad + \ldots\ldots + \sum_{\tau=0}^{\mu} h_{yx_i}(\tau)E[x_1(t-k)x_i(t-\tau)] \\ &\quad + \ldots\ldots + \sum_{\tau=0}^{\mu} h_{yx_N}(\tau)E[x_1(t-k)x_N(t-\tau)] \end{aligned}$$

This is the first of the set of simultaneous equations, which when solved yield the unknown response functions. By repeating this process for each input channel, i.e multiplying equation (1) by $x_r(t-k)$,where r denotes an arbitrary input channel (which varies between 2 and N), and the application of the expectation operator, we obtain,

$$\begin{aligned} E[x_2(t-k)y(t)] &= \sum_{\tau=0}^{\mu} h_{yx_1}(\tau)E[x_2(t-k)x_1(t-\tau)] + \sum_{\tau=0}^{\mu} h_{yx_2}(\tau)E[x_2(t-k)x_2(t-\tau)] \\ &\quad + \ldots\ldots + \sum_{\tau=0}^{\mu} h_{yx_i}(\tau)E[x_2(t-k)x_i(t-\tau)] \\ &\quad + \ldots\ldots + \sum_{\tau=0}^{\mu} h_{yx_N}(\tau)E[x_2(t-k)x_N(t-\tau)] \end{aligned}$$

$$E[x_3(t-k)y(t)] = \sum_{\tau=0}^{\mu} h_{yx_1}(\tau)E[x_3(t-k)x_1(t-\tau)] + \sum_{\tau=0}^{\mu} h_{yx_2}(\tau)E[x_3(t-k)x_2(t-\tau)]$$
$$+ \ldots\ldots + \sum_{\tau=0}^{\mu} h_{yx_i}(\tau)E[x_3(t-k)x_i(t-\tau)]$$
$$+ \ldots\ldots + \sum_{\tau=0}^{\mu} h_{yx_N}(\tau)E[x_3(t-k)x_N(t-\tau)]$$

and so on. This set of equations can be written in the following general form,

$$E\left[x_r(t-k)y(t)\right] = \sum_{i=1}^{N}\sum_{\tau=0}^{\mu} h_{yx_i}(\tau)E\left[x_r(t-k)x_i(t-\tau)\right] \tag{2}$$

By denoting the second order cross moment between the rth input channel and the output, $E[x_r(t-k)y(t)]$, as $M_{x_ry}(k)$, and the second order cross moment between the rth and ith input channels, $E[x_r(t-k)x_i(t-\tau)]$, as $M_{x_rx_i}(k,\tau)$, equation (2) can be written in the following form,

$$M_{x_ry}(k) = \sum_{i=1}^{N}\sum_{\tau=0}^{\mu} h_{yx_i}(\tau)M_{x_rx_i}(k,\tau)$$

This yields a set of simultaneous equations over all the input channels and over the length of the 'memory' of the system, explicitly this means we obtain, from this set of simultaneous equations, the form of a $\mathbf{A}x = b$ matrix equation,

$$\begin{bmatrix} M_{x_1y}(k) \\ M_{x_2y}(k) \\ \vdots \\ M_{x_Ny}(k) \end{bmatrix} = \begin{bmatrix} M_{x_1x_1}(k,\tau) & M_{x_1x_2}(k,\tau) & \ldots\ldots & M_{x_1x_N}(k,\tau) \\ M_{x_2x_1}(k,\tau) & M_{x_2x_2}(k,\tau) & \ldots\ldots & M_{x_2x_N}(k,\tau) \\ \vdots & \vdots & \vdots & \vdots \\ M_{x_Nx_1}(k,\tau) & M_{x_Nx_2}(k,\tau) & \ldots\ldots & M_{x_Nx_N}(k,\tau) \end{bmatrix} \begin{bmatrix} h_{yx_1}(\tau) \\ h_{yx_2}(\tau) \\ \vdots \\ h_{yx_N}(\tau) \end{bmatrix} \tag{3}$$

Each term in these general matrices represents a number of elements in the **A** and b matrices (as k and τ vary between 0 and μ), within the $\mathbf{A}x = b$ equation which is solved using standard matrix methods for the unknown impulse response functions values, $h_{yx_i}(\tau)$. If N is set to 1 then a single input analysis is performed.

The methodology presented here is quite general, and may be applied to a wide range of problems, we shall consider a specific application of the technique to the analysis of the heat transfer processes within buildings. However before we apply this novel tecchnique to the analysis of real experimental data, we shall consider a numerical experiment with computer generated data, in which the properties of the system are known.

Numerical experiment using computer generated data

In this section, the results from a numerical experiment, where the properties of the linear multi-input system are known, are presented. A numerical experiment is used so that the accuracy and range of appropriate use of the technique in the estimation of the impulse response functions of a multi-input system can be assessed, through the comparison of the estimated, $h_{yx_i}(t)$ and known, $g_{yx_i}(t)$, response functions. This comparison will be performed on the basis of two statistical metrics, the root mean square and absolute mean differences between the known and estimated impulse response functions, where the root mean square difference, for the ith input channel, is given by,

$$\text{rms}_i = \sqrt{\left[\frac{1}{\mu+1}\sum_{\tau=0}^{\mu}(h_{yx_i}(\tau) - g_{yx_i}(\tau))^2\right]} \tag{4}$$

and the absolute mean difference by,

$$\text{abs diff}_i = \frac{1}{\mu+1}\sum_{\tau=0}^{\mu} \mid (h_{yx_i}(\tau) - g_{yx_i}(\tau)) \mid \tag{5}$$

These two statistical metrics will demonstrate, whether or not, the technique can correctly estimate the known response functions to a high degree of accuracy.

In this example we use a three input - one output system, such that $N = 3$ in equation (1), and the known linear impulse response functions are given by,

$$\begin{aligned} g_{yx_1}(\tau) &= e^{-0.5*\left(\frac{\tau-5}{3}\right)^2} \\ g_{yx_2}(\tau) &= e^{-0.3\tau} * \cos(\pi * \tau/5) \\ g_{yx_3}(\tau) &= e^{-0.3\tau} \end{aligned} \tag{6}$$

The inputs to this system are taken from the experimentally measured time series values of the wind speed, $ws(t)$, and heat flux at the internal surface of the ceiling, $q(t)$, from the data set described in the next section. The input time series for each of the first two channels of the system is convolved from the wind speed data, such that

$$x_1(t) = 0.5ws(t) + 0.75ws(t-1) + 0.6ws(t-2) + 0.55ws(t-3) + 0.5ws(t-4) + 0.43ws(t-5) + 0.4ws(t-6) + 0.35ws(t-7) + 0.3ws(t-8) + 0.2ws(t-9) + 0.15ws(t-10) + 0.1ws(t-11) + 0.05ws(t-12) - 0.05ws(t-13) - 0.1ws(t-14) - 0.15ws(t-15) - 0.2ws(t-16) - 0.1ws(t-17) - 0.05ws(t-18) - 0.05ws(t-19) - 0.03ws(t-20) - 0.01ws(t-21)$$

$$x_2(t) = 1.0ws(t) + 0.7ws(t-1) + 0.6ws(t-2) + 0.5ws(t-3) + 0.4ws(t-4) + 0.35ws(t-5) + 0.3ws(t-6) + 0.2ws(t-7) + 0.17ws(t-8) + 0.14ws(t-9) + 0.12ws(t-10) + 0.08ws(t-11) + 0.06ws(t-12) + 0.05ws(t-13) - 0.05ws(t-14) - 0.1ws(t-15) - 0.2ws(t-16) - 0.24ws(t-17) - 0.15ws(t-18) - 0.06ws(t-19) - 0.03ws(t-20) + 0.01ws(t-21)$$

Thus there will be a strong correlation between two of the input channels to the system. The input to the third channel is the unmodified surface heat flux time series data i.e $x_3(t) = q(t)$. Typical samples of the three input time series are shown in figures 1, 2 and 3. The close correlation between two of the inputs can be observed from a comparison of figures 1 and 2 (i.e samples of the input data to channels one and two). Figure 4 shows a sample of the output data generated using equation (1), with this input data and the known response functions given by equation (6).

The analysis is performed using 1000 points of time series data, and a maximum time delay of 20, i.e $\mu = 20$. Figures 5 and 6 show the estimated linear response function for the first input channel, $h_{yx_1}(t)$, and the differences between the estimated and known response function values for this channel, $(h_{yx_1}(t) - g_{yx_1}(t))$. The differences of 10^{-7} are not untypical of the accuracy of the technique for numerical studies. Figures 7 and 9 show the estimated linear response functions for the second and third input channels, while figures 8 and 10 show the differences between the estimated and known response functions for these channels. Table 1 presents the area under the estimated and known response functions, and the root mean square and absolute mean differences between the estimated and known response functions, given by equations (4) and (5). [Note the area under a response function is given by $\sum_{\tau=0}^{\mu} h_{yx}(\tau)$].

The RMS and absolute mean differences of at least 10^{-7} demonstrate the ability and accuracy of this new technique. This example has demonstrated that the technique can correctly estimate the response functions of a multi-input system, even when two of the inputs to the system are highly correlated.

Experimental data

The experimental data set used in the present work was collected, from the British Gas plc test cell at Cranfield, by the Energy Monitoring Company (EMC), over the 1989/90 heating season [6]. The test cell has internal dimensions of 2.03m by 2.03m by 2.33m tall. The four walls of the test cell, which are of a externally insulated brick construction, are built off an insulated timber floor panel which has been raised on blocks above ground level, allowing the floor panel to be at the ambient external temperature. The flat roof of the test cell is of a timber-frame styrofoam construction, with waterproofed plywood as the external surface and plasterboard as the internal surface. The internal surfaces of the test cell are finished with a coat of matt white paint.

The test cell is exposed to natural external meteorological conditions, however no solar radiation is directly incident on any of the interior surfaces of the test cell. It is very highly sealed, as the natural infiltration rate was less than 0.05 ac/hr, as determined from a pressure test on the building [6]. The test cell was continuously mechanically ventilated by the outside air, ducted via a pulse output gas meter, to record the ventilation rate, which was set at approximately 2 ac/hr using dampers on the inlet and outlet ducts. This air entered the test cell via a diffuser pipe, running from the floor to the ceiling, in the north-west corner. The velocity in the diffuser pipe can be determined from the diameter of the pipe and the air change rate, and was approximately 0.7 m/s. The air, within the test cell, was heated by a 1 kW convective heater, controlled by a pseudo random sequence of on/off pulses with a 5 minute time step.

Time series data were collected at 5 minute intervals for a period of 20 days for the experiment. External meteorological measurements were obtained for the dry bulb temperature, wind speed and direction, and the global and diffuse horizontal irradiance. Internal

measurements were obtained for various air and surface temperatures, and for the heat flux at each surface. In order to estimate the surface heat transfer coefficient, a Meyer ladder [7] was employed, this measures the air temperature through the boundary layer, from the surface to which it is attached to the bulk air. A ladder consists of a set of air temperature sensors (in this case ten) at accurately defined distances from the surface, a free stream air temperature sensor, and a surface temperature sensor. In this experiment the ladder was mounted on the ceiling of the test cell in the proximity of the heat flux mat on this surface.

Application of technique

The new technique for the estimation of the response functions from multi-input systems presented in this work, will now be employed to investigate the energy balance at the surface of the ceiling in the test cell described in the previous section. The energy balance across a volume enclosing the surface can be written as,

$$q(t) = q_{conduction}(t) + q_{radiation}(t) + q_{convection}(t) \tag{7}$$

such that the oberserved heat flux at the surface, $q(t)$, is composed of components due to the conductive, radiative and convective processes that interact at the surface. This equation can be written in terms of the physical observable variables and the linear response factors or functions of each process as,

$$q(t) = \sum_{\tau=0}^{\mu} h_{q\Delta T_s}(\tau)\Delta T_s(t-\tau) + \sum_{\tau=0}^{\mu} h_{q\Delta T_r^4}(\tau)\sigma\Delta T_r^4(t-\tau) + \sum_{\tau=0}^{\mu} h_{q\Delta T_f}(\tau)\Delta T_f(t-\tau) \tag{8}$$

where $\{\Delta T_s(t), \Delta T_r^4(t), \Delta T_f(t)\}$ are, respectively, the temperature gradient within the ceiling, the difference between the fourth powers of the surface temperatures of the ceiling and the average of the remaining surfaces within the test cell, and the temperature difference across the air-surface boundary layer, and where $h_{q\Delta T_s}(\tau), h_{q\Delta T_r^4}(\tau), h_{q\Delta T_f}(\tau)$ are, respectively the response factors for the conductive, radiative and convective processes. (σ is the Stefan-Boltzmann constant, and is equal to $56.7 * 10^{-9}\mathrm{W/m^2K^4}$). The cubic geometry of the test cell and the fact that all the surfaces within the test cell were finished with a

coat of matt white paint mean that no account need be taken of the radiative view factors and the emissivity of each surface. The area under the estimated response factors for each process is the heat transfer coefficient or gain of that process [8].

However, the construction of the test cell, i.e the layer of styrofoam on the external surface, means that the test cell has a time constant for the conductive path of the order of days, and so this path will be assumed to be negligible when compared with either the convective or radiative flowpaths. Hence equations (7) and (8) can be re-written as,

$$q(t) = q_{radiation}(t) + q_{convection}(t)$$

and,

$$q(t) = \sum_{\tau=0}^{\mu} h_{q\Delta T_r^4}(\tau)\sigma\Delta T_r^4(t-\tau) + \sum_{\tau=0}^{\mu} h_{q\Delta T_f}(\tau)\Delta T_f(t-\tau)$$

From this point in the work, the Stefan-Boltzmann constant, σ, will be combined with the difference between the fourth powers of the surface temperatures of the ceiling and the average of the remaining surfaces within the test cell, $\Delta T_r^4(t-\tau)$. Following the novel methodology presented in this work, we may take time series moments between the heat flux at the ceiling surface and the two temperature differences $\Delta T_r^4(t-\tau), \Delta T_f(t-\tau)$, to give

$$M_{\Delta T_r^4 q}(k) = \sum_{\tau=0}^{\mu} h_{q\Delta T_r^4}(\tau) M_{\Delta T_r^4 \Delta T_r^4}(k,\tau) + \sum_{\tau=0}^{\mu} h_{q\Delta T_f}(\tau) M_{\Delta T_r^4 \Delta T_f}(k,\tau)$$

$$M_{\Delta T_f q}(k) = \sum_{\tau=0}^{\mu} h_{q\Delta T_r^4}(\tau) M_{\Delta T_f \Delta T_r^4}(k,\tau) + \sum_{\tau=0}^{\mu} h_{q\Delta T_f}(\tau) M_{\Delta T_f \Delta T_f}(k,\tau)$$

Thus there are $2 * (\mu + 1)$ simultaneous equations, which is equal to the number of unknown response function values. These equations can be written in matrix form, similar to equation (3), to give,

$$\begin{bmatrix} M_{\Delta T_r^4 q}(k) \\ M_{\Delta T_f q}(k) \end{bmatrix} = \begin{bmatrix} M_{\Delta T_r^4 \Delta T_r^4}(k,\tau) & M_{\Delta T_r^4 \Delta T_f}(k,\tau) \\ M_{\Delta T_f \Delta T_r^4}(k,\tau) & M_{\Delta T_f \Delta T_f}(k,\tau) \end{bmatrix} \begin{bmatrix} h_{q\Delta T_r^4}(\tau) \\ h_{q\Delta T_f}(\tau) \end{bmatrix}$$

where $M_{\Delta T_r^4 q}, M_{\Delta T_f q}$ are the cross time series moments between the two inputs (the temperature differences) and the output (the surface heat flux), and

$M_{\Delta T_r^4 \Delta T_r^4}, M_{\Delta T_r^4 \Delta T_f}, M_{\Delta T_f \Delta T_r^4}, M_{\Delta T_f \Delta T_f}$ are the auto and cross time series moments between the two inputs. This set of simultaneous equations are solved, for the unknown response functions, using standard matrix methods.

These estimated response functions characterise the convective and radiative processes that contribute to the observed heat flux, taking account of any correlation between the two processes. That is, the technique allows for the fact that one process may be 'driving' the other, hence the inputs are not strictly independant, if this is the case then the results from a single-input analysis may be questionable. Any correlation between the two inputs will be shown in the cross-covariance function, $M_{\Delta T_r^4 \Delta T_f}(k, \tau)$, this function will also enable the 'driven' process, if any, to be identified. The area under the estimated first order/linear response function is the linear steady state gain of that process [8]. The steady state gain between the surface heat flux and the temperature difference driving force of a process is the surface heat transfer coefficient of that process [5].

Analysis of experimental data

I : VECTOR INPUT APPROACH

In this section the novel technique for the estimation of the impulse response functions of multi-input systems presented in this work, will be applied to the experimental data set previously described [6]. The response functions for the convective and radiative processes acting at the ceiling of the test cell will be estimated from the time series data. The convective and radiative heat transfer coefficients, for the ceiling of the test cell, will be determined as the area under the estimated response function for each process. In addition the Meyer ladder will enable an investigation into the thickness of the air boundary layer at the ceiling to be performed. The results from the multi-input analysis of the data will also be compared with those obtained from single-input analyses, and conclusions drawn regarding the necessity for the inclusion of all input variables or boundary conditions in the analysis of any process.

Figure 11 shows a typical 24 hour sample of the temperature difference between a typical (the eighth) Meyer ladder sensor and the surface of the ceiling. Figure 12 shows the differ-

ence between the fourth powers of the surface temperature of the ceiling and the average temperature of the remaining surfaces within the test cell, allowing for the Stefan-Boltzmann constant, for the same 24 hour period. Figure 13 shows the corresponding 24 hour sample of the heat flux at the ceiling surface, shown as positive with heat flow into the surface.

The response functions for the convective and radiative processes, from which the convective and radiative heat transfer coefficients are determined, were estimated from a sequence of 1440 points (i.e 5 days) of time series data, for each of the ten Meyer ladder sensors. The maximum length of time delay or the length of the memory of the processes, μ, was set to 3 hours. Table 2 presents the convective and radiative heat transfer coefficients estimated for each Meyer ladder sensor, calculated as the area under the estimated response function for each process at each Meyer ladder sensor.

Figure 14 shows the estimated linear response function of the surface heat flux to the temperature difference between the eighth Meyer ladder sensor and the surface of the ceiling. The area under this curve is the convective heat transfer coefficient between the ceiling and the air around the eighth sensor, and is $3.859 W/\mathrm{m}^2 K$. Figure 15 shows the corresponding estimated linear response function of the surface heat flux to the difference between the fourth powers of the surface temperature of the ceiling and the average temperature of the remaining surfaces. The area under this curve is the radiative heat transfer coefficient, which for the eighth Meyer ladder sensor is 0.382.

Figure 16 shows the convective and radiative heat transfer coefficients for each Meyer ladder sensor across the air-surface boundary layer at the ceiling, using a logarithmic scale for the distance of each sensor from the surface of the ceiling. The convective heat transfer coefficient between the ceiling and the bulk air within the test cell is the asymptotic value of the convective heat transfer coefficient curve and is approximately $3.8 W/\mathrm{m}^2 K$. The thickness of the boundary layer at the ceiling can be estimated from this curve, as the point at which the convective HTC is approximately this asymptotic value, and hence in this experiment, the thickness of the boundary layer is approximately 50 mm. The radiative heat transfer coefficient can be observed to be approximately constant, as would be expected, and has a value of approximately 0.4 . The consistency of the estimate of the radiative heat transfer coefficient across the air-surface boundary layer, despite the variation of the convective heat

transfer coefficient estimate, should be noted.

II : SINGLE INPUT APPROACH

The same period of data as employed in the multi-input analyses for the each Meyer ladder sensor was also used in the single-input analyses. In these single-input analyses, it is assumed that all the boundary conditions (or inputs) are independant, and are, hence, uncorrelated with each other. As in the multi-input analyses, the maximum length of time delay was set to 3 hours (36 points).

In the first set of single-input analysis, the convective heat transfer coefficient between the air and the ceiling surface will be estimated. Figures 11 and 13 show typical 24 hour samples of the temperature difference between the eighth sensor on the ladder and the surface of the ceiling, and the corresponding sample of the heat flux at the ceiling surface. Figure 17 shows the estimated linear response function of the surface heat flux to the air-surface temperature difference, from a single-input analysis. The area under the estimated response function of the surface heat flux to the temperature difference between the eighth ladder sensor and the ceiling surface, or the convective heat transfer coefficient, is $2.328 W/\mathrm{m}^2 K$. Table 3 presents the convective heat transfer coefficients estimated at each Meyer ladder sensor, by the single-input approach.

A single analysis employing the single-input approach to estimate the radiative heat transfer coefficient between the ceiling and the other surfaces within the test cell was performed. Figures 12 and 13 show typical 24 hour samples of the difference between the fourth powers of the surface temperature of the ceiling and the average temperature of the remaining surfaces within the test cell and the corresponding sample of the heat flux at the ceiling surface. Figure 18 shows the estimated linear response function of the surface heat flux to the difference between the fourth powers of the surface temperature of the ceiling and the average temperature of the remaining surfaces within the test cell. The area under the estimated response function, or the radiative heat transfer coefficient is -0.55.

Single-input vs. Multi-input comparison

A comparison of the convective heat transfer coefficients determined, as the area under the estimated response function from the single- and multi- input approaches, show that the single-input approach yields a lower estimate of the convective heat transfer coefficient than the multi-input approach, by about 50 per cent. The estimated response functions from the two approaches, shown in figures 14 and 17, are similar in form, however after an initial peak in both cases (which are different in magnitude) the single-input approach estimates a long negative tail in the response function, whereas the multi-input approach estimates a noisy tail with an aproximate zero mean.

A comparison of the radiative heat transfer coefficients determined from the single- and multi- input approaches show that the two approaches yield positive and negative values for the radiative heat transfer coefficients. It can be observed that this quantity should be postive due to the directions of surface-surface temperature difference and the heat flux at the ceiling, this is as inferred by the multi-input approach. Thus the single-input approach gives a mis-leading result in this case. This is despite the estimated response functions being similar in form, as can be observed from figures 15 and 18.

The differences between the convective and radiative heat transfer coefficients estimated, by the single- and multi- input approaches, can be explained by considering the correlation between the two inputs, i.e the air-surface and surface-surface temperature differences. Figure 19 shows the second order cross covariance between the air-surface and surface-surface temperature differences. It can be observed from this figure that the covariance function between the two input channels is not symmetrical along the $\tau 1 = \tau 2$ diagonal, and that the convective process is driving the radiative process, as indicated by the region where $\tau 1 > \tau 2$. By comparing this figure to figures 20 and 21, which show the second order auto covariance of the air-surface and surface-surface temperature differences, it can be observed that the cross-covariance is of the same order of magnitude as the auto covariance functions. As such this will affect the response functions estimated for the convective and radiative processes, by the single-input formalism employed in this work.

The difference between the results obtained using the single- and multi- input analysis

approaches from a multi-input system is clearly shown by employing the estimated response functions of the convective and radiative processes and the driving forces to predict the heat flux at the ceiling surface. Figures 22 and 23 show the measured and predicted surface heat flux for the multi- and single- input formalisms, respectively. It can be seen from these figures that due to the correlation between the convective and radiative driving forces, the estimated response functions from the single-input analysis over predicts the surface heat flux. Figure 24 shows the same sample of predicted heat flux, as that shown in figure 22, split into it's convective and radiative components, as predicted from the response functions for the convective and radiative processes estimated by the multi-input formalism. This figure indicates that the convective process is predominantly 'driving' heat into the ceiling, whereas the radiative process is removing heat. This figure also shows that the components of the surface heat flux due to the convective and radiative processes are similar in magnitude, despite there being a 10:1 (convective : radiative) ratio in their estimated heat transfer coefficients.

Conclusions

A new technique for the estimation of the vector linear response functions from the time series of a multi-input system, that allows for correlation between the time series inputs has been presented. The technique is a time series method, and is based upon the observed correlation between the experimentally observed values and the impulse response functions, which are characterisations of the physical relationships between the input-output variables. The ability of this novel technique to correctly estimate the response functions of a multi-input system is demonstrated, using a numerical example. In this numerical example, where the properties of the system are known, the technique is shown to estimate the response functions of the system to a high degree of accuracy.

The technique is then applied to analyse time series data collected from a well insulated, single zone experimental building. The technique is employed to estimate the response functions of the coupled convective / radiative processes that act at the internal surface of the ceiling of the building. The area under the estimated response function of each process is the heat transfer coefficient of that process. These show the convective heat transfer

coefficient between the ceiling surface and the bulk air within the single zone building to be approximately $3.8W/\mathrm{m}^2K$, and the radiative heat transfer coefficient between the ceiling surface and the other surfaces within the zone to be approximately 0.4 . These values agree well with currently used empirical ones. The form of the estimated response function of each process has demonstrated that both the convective and radiative processes acting at an internal surface have a short term 'memory' of about 10 minutes. That is the heat flux, at the current time, is predominantly affected by the convective and radiative driving forces of up to 10 minutes ago. The thickness of the air boundary layer at the internal surface of the ceiling has also been estimated and is approximately 50 mm.

The response functions and heat transfer coefficients estimated by the multi-input approach, presented in this paper, were compared with those obtained from a single-input approach. This comparison showed that eventhough the estimated response functions were similar in form, they differed in magnitude, and that the estimated heat transfer coefficient for each process, determined from the estimated response function, were different between the two approaches. The differences between the single- and multi- input approaches were more clearly shown by employing the estimated response functions and the driving forces of each process, to predict the heat flux at the ceiling surface. This demonstrated that the response functions from the single-input approach over predict the heat flux at the ceiling surface, whereas the response functions from the multi-input approach correctly predict the heat flux. This is due to the correlation between the driving forces of the convective and radiative processes, which is accounted for in the multi-input approach, but not in the single-input approach. It has been shown, by considering the correlation function between the convective / radiative driving forces, that the convective process is driving the radiative process, in this experimental situation.

In general, this work has demonstrated that in order to obtain a valid mathematical model of the system under investigation, it is necessary to consider all the inputs to or driving forces of the system, and to employ a multi-input analysis technique, to allow for any correlation / dependance between the inputs to the system.

Acknowledgments

This work was supported by the Building Sub-Committee of the UK Science and Engineering Research Council. The authors would like to express their thanks to the Energy Monitoring Company who collected and supplied the field data, and to British Gas Plc who funded the data collection.

References

[1] Box GEP and Jenkins GM, Time Series Analysis - Forecasting and Control, Holden-Day, San Francisco, 1976.

[2] Priestley MB, Spectral Analysis and Time Series, Academic Press, London, 1981.

[3] Irving AD, Dewson T, Hong G and Cunliffe N, Nonlinear Response Function Estimation I : Mixed order case, In press Applied Mathematical Modelling, November 1994. [also Rutherford Appleton Laboratory report RAL-91-067].

[4] Newland DE, An introduction to Random Vibrations and Spectral Analysis, Longman, London, 1975.

[5] Irving AD, Dewson T, Hong G and Day B, Time Series Estimation of Convective Heat Transfer Coefficients, Building and Environment, Vol 29 No 1 pp89-96, 1994.

[6] Martin C and Watson M, Further Experiments in a Highly Instrumented Test Room, Energy Monitoring Company report and data set, Private communication, 1990.

[7] Delaforce S, Hitchin ER and Watson M, Private communication, 1992.

[8] Irving AD, Stochastic Sensitivity Analysis, Applied Mathematical Modelling 16, 1992.

Input Channel	Estimated Area	Theoretical Area	RMS difference	Absolute mean difference
1	7.2736401	7.2736336	$5.717*10^{-7}$	$4.349*10^{-7}$
2	1.1439284	1.1439354	$5.591*10^{-7}$	$4.423*10^{-7}$
3	3.8512109	3.8512109	$2.681*10^{-11}$	$2.275*10^{-11}$

Table 1: Results from the numerical experiment using computer gernerated data

Sensor Number	Convective HTC (W/m^2K)	Radiative HTC
1	8.992	0.363
2	6.519	0.383
3	5.495	0.404
4	5.203	0.420
5	4.379	0.410
6	4.168	0.402
7	3.968	0.392
8	3.859	0.382
9	3.820	0.378
10	3.948	0.379

Table 2: Convective and Radiative heat transfer coefficients for each Meyer ladder sensor, from the multi-input approach

Sensor Number	Convective HTC (W/m^2K)
1	5.532
2	3.926
3	3.329
4	3.016
5	2.565
6	2.462
7	2.369
8	2.328
9	2.315
10	2.439

Table 3: Convective heat transfer coefficient for each Meyer ladder sensor, by the single-input approach

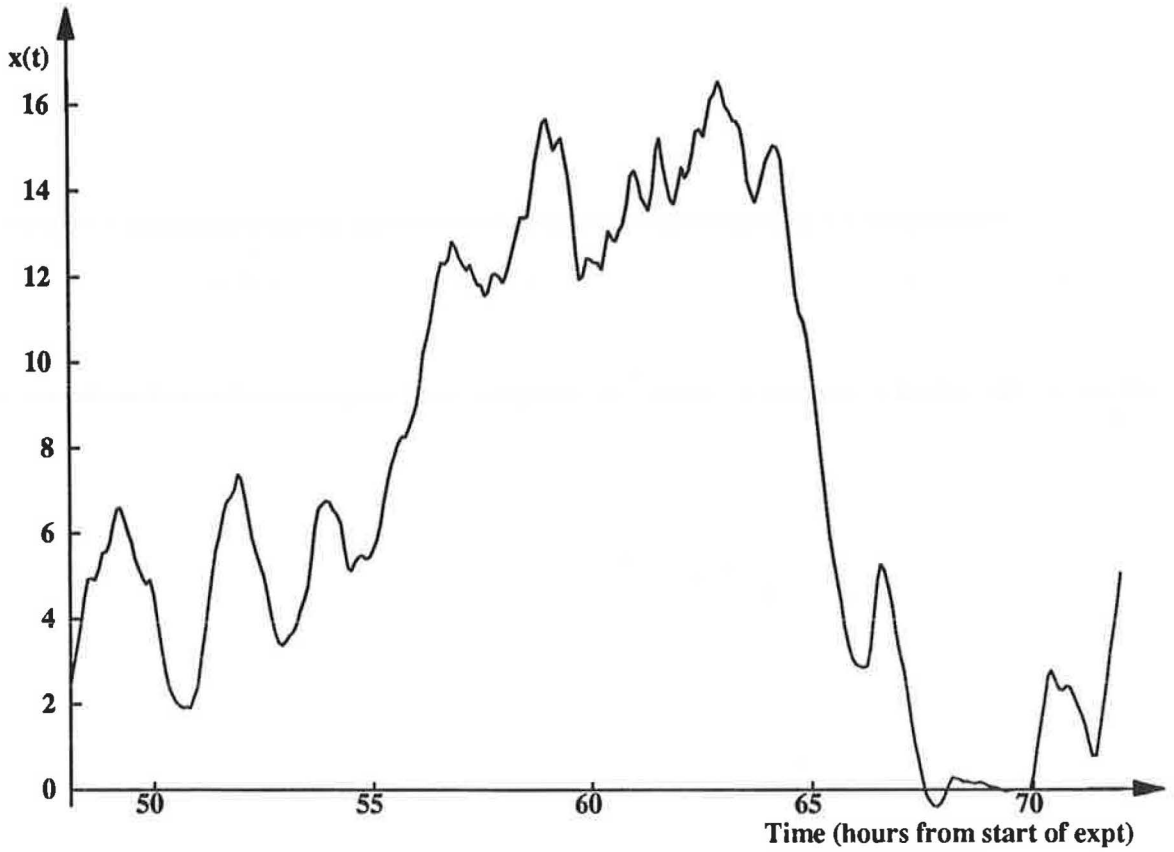

Figure 1 : A sample of the input time series on channel one, which has been convolved from the wind speed time series data

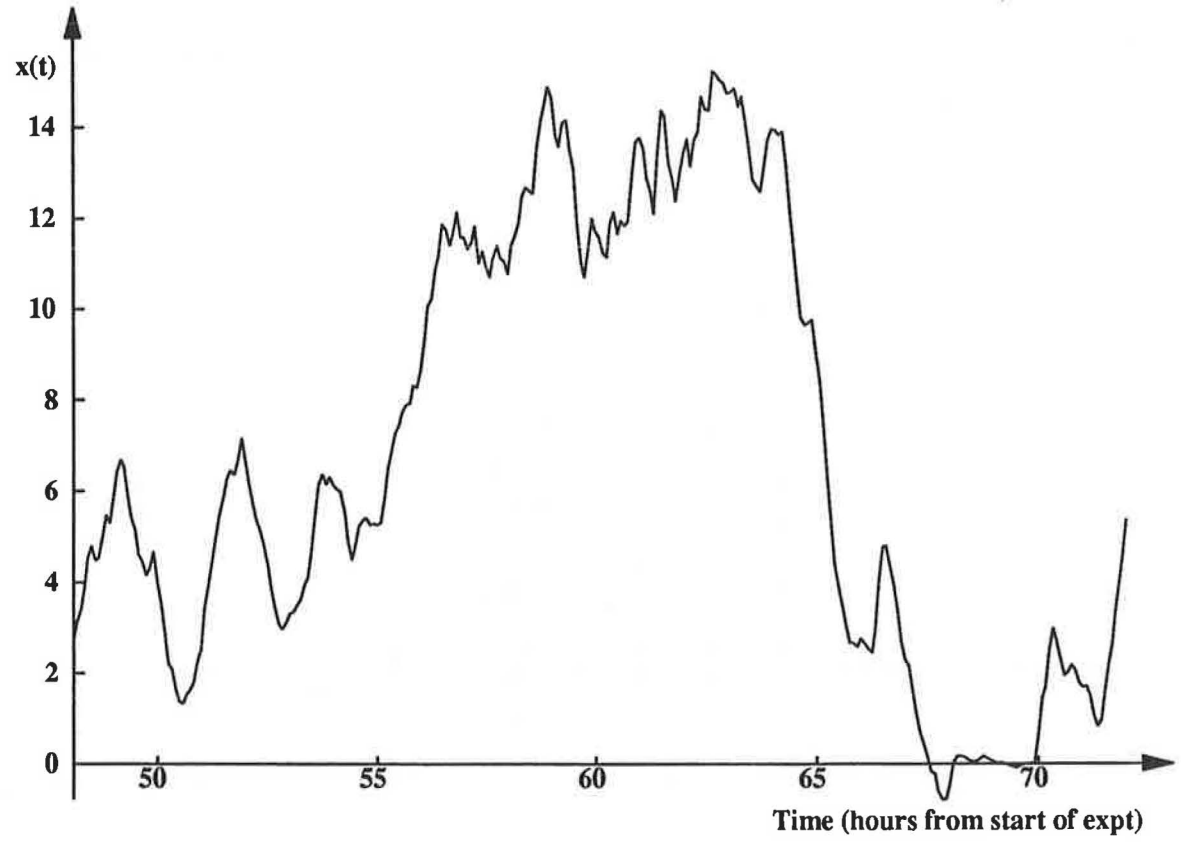

Figure 2 : A sample of the input time series on channel two, which has been convolved from the wind speed time series data

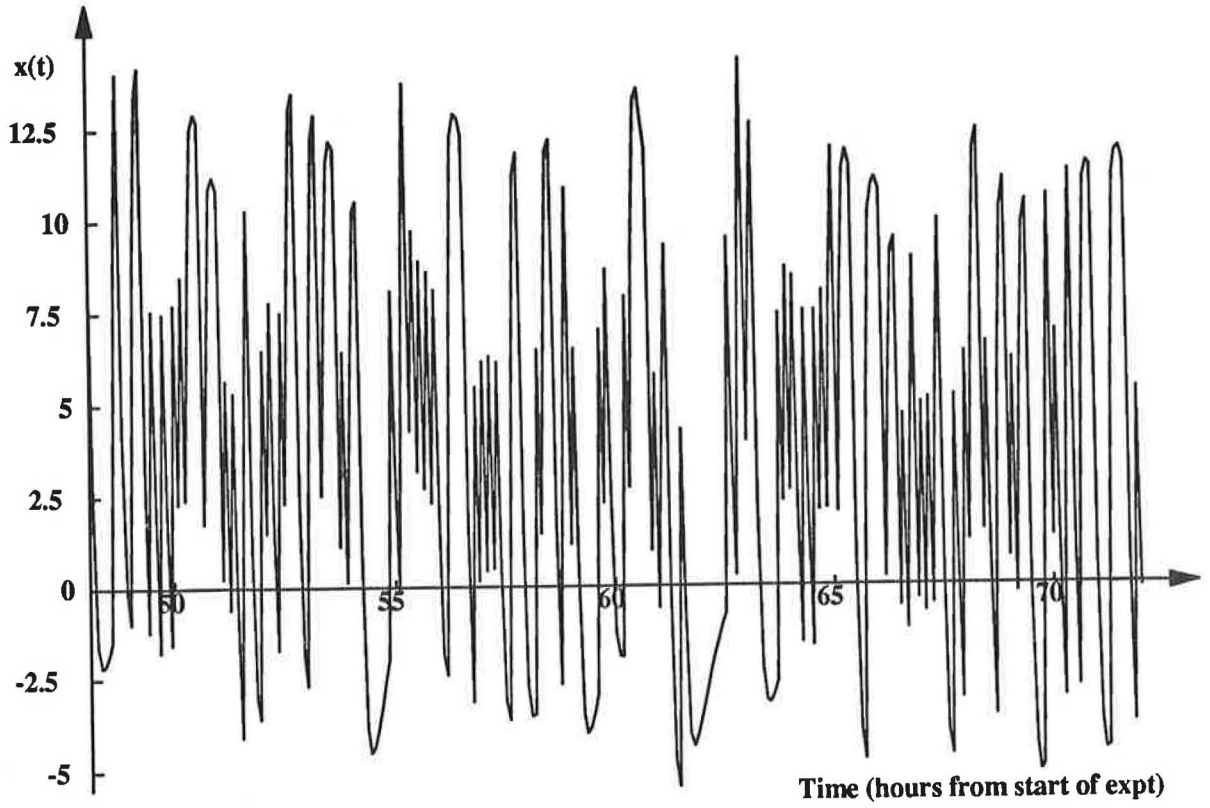

Figure 3 : A sample of the input time series on channel three

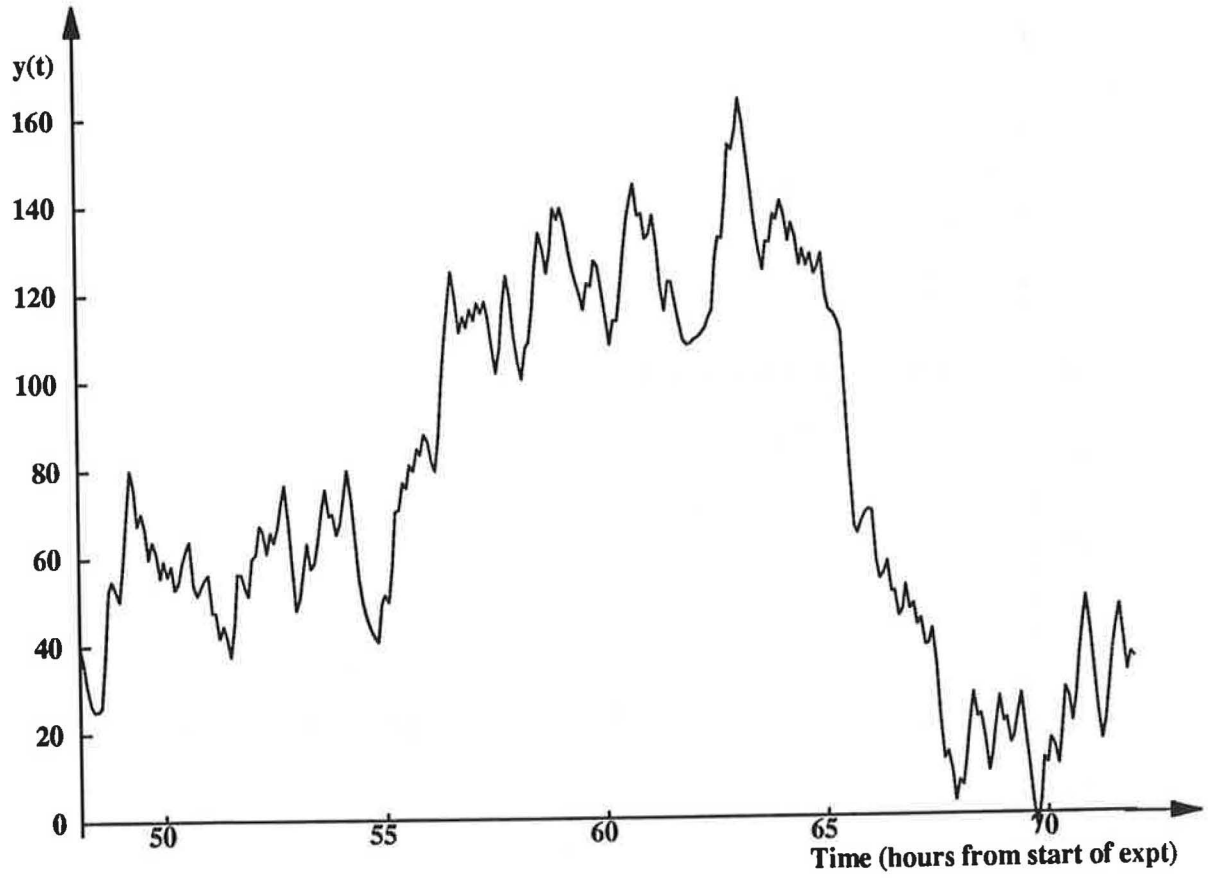

Figure 4 : The corresponding sample of output data generated using the known response functions and the data on the three input channels

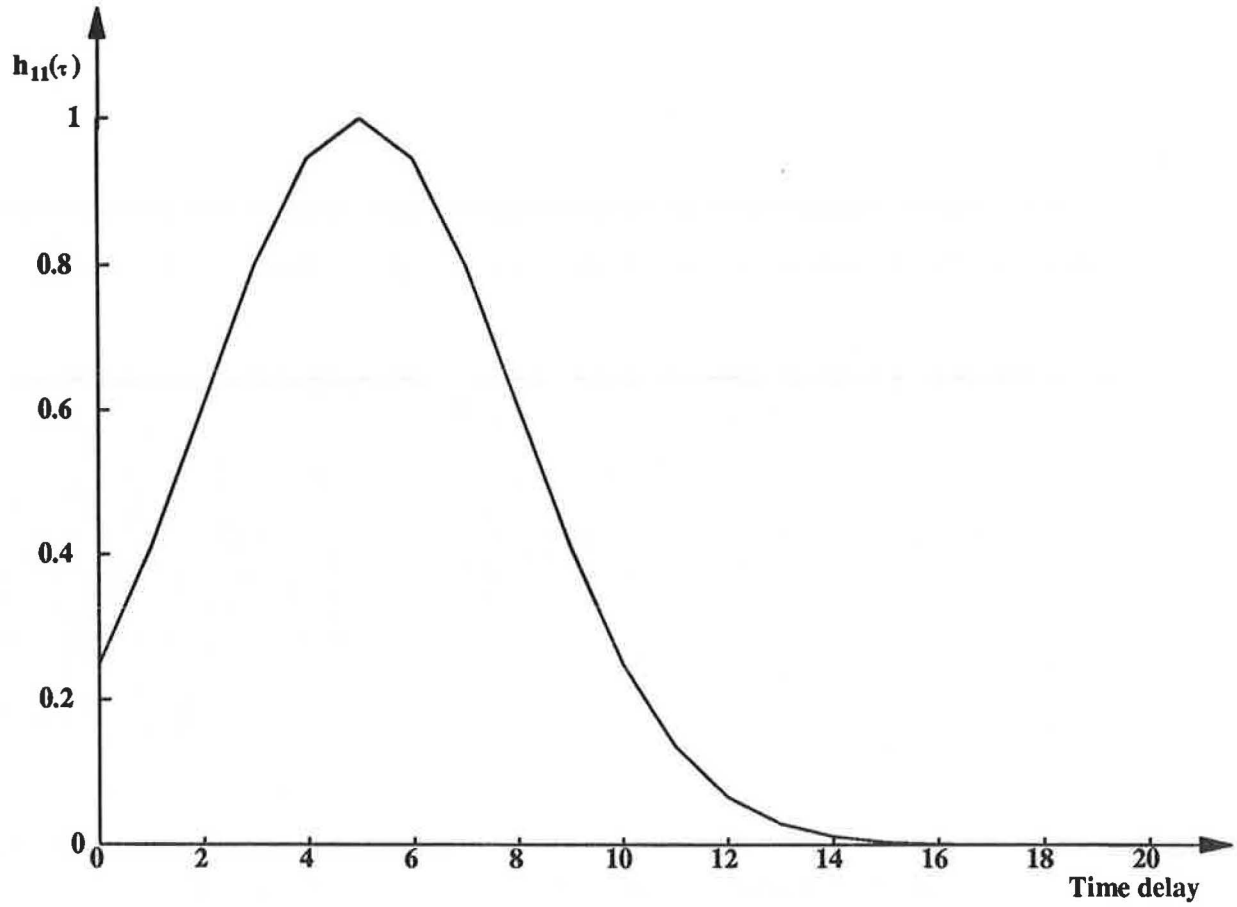

Figure 5 : The estimated linear response function for the first input channel

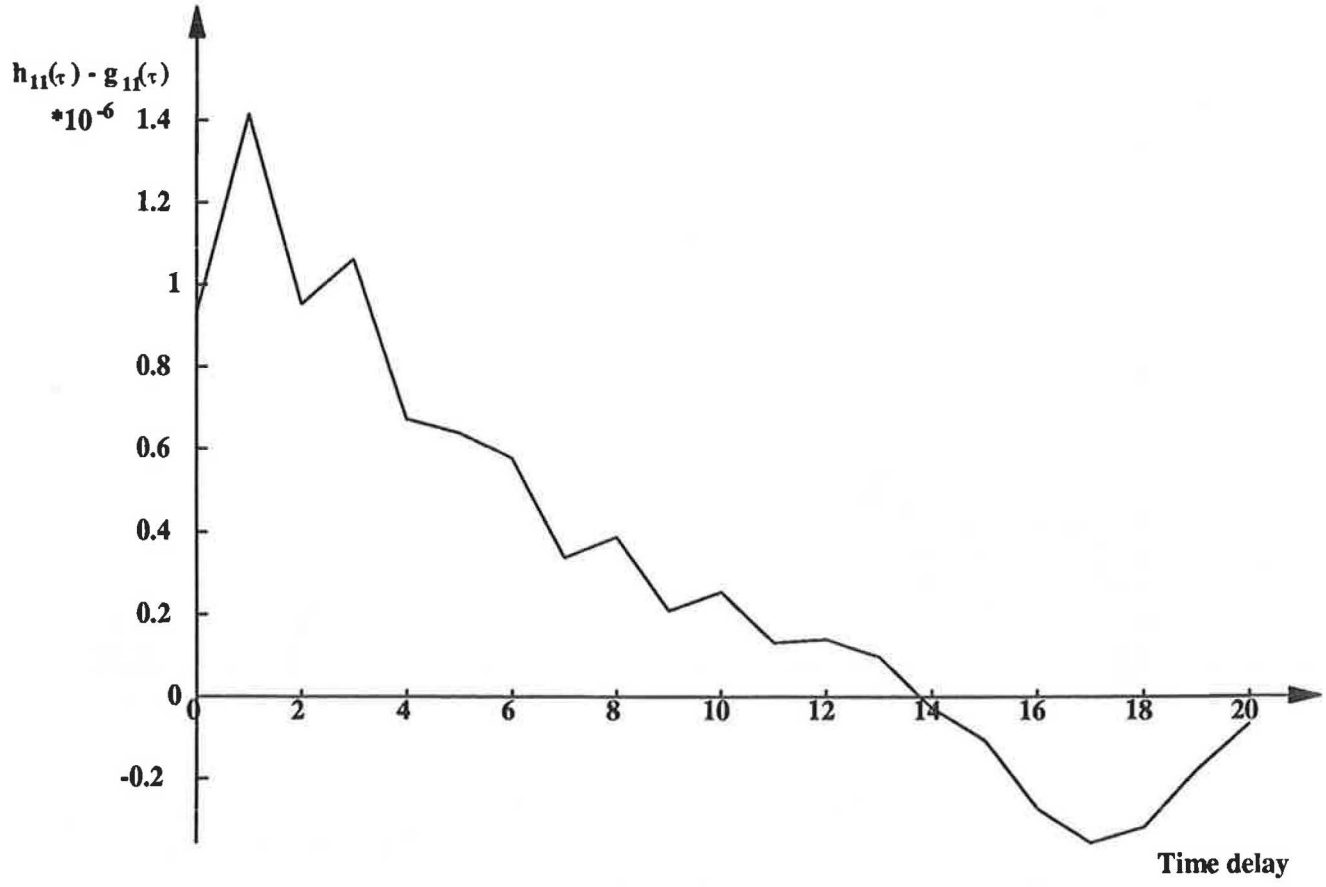

Figure 6 : The difference between the estimated and known linear response functions for the first input channel

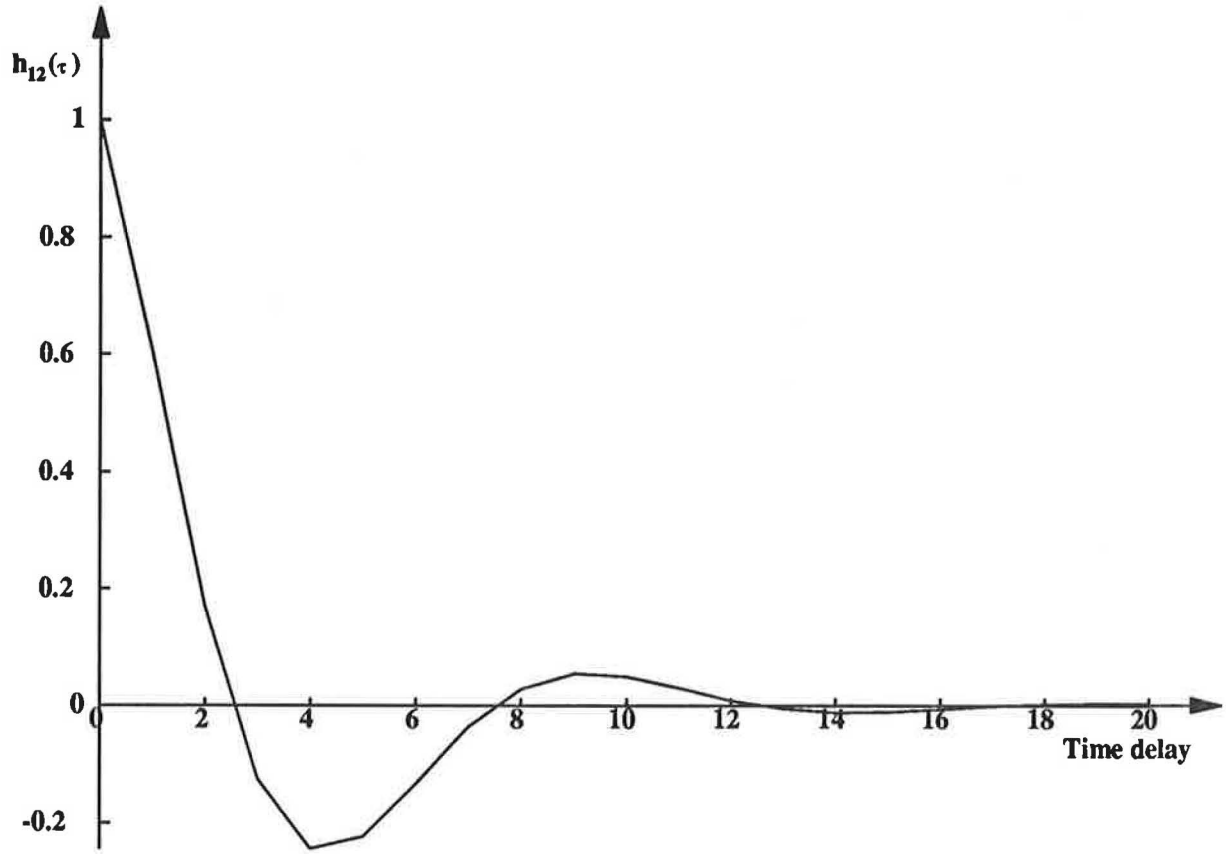

Figure 7 : The estimated linear response function for the second input channel

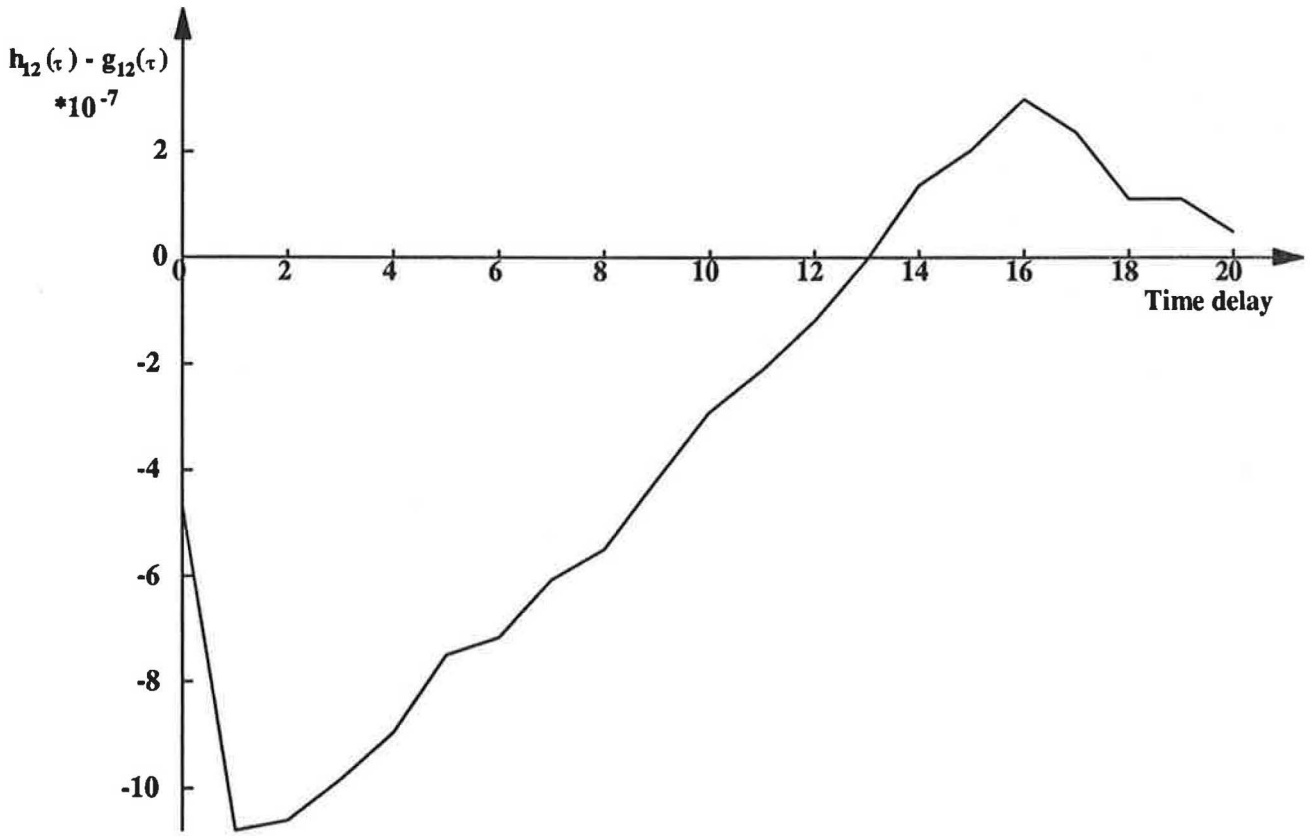

Figure 8 : The difference between the estimated and known linear response functions for the second input channel

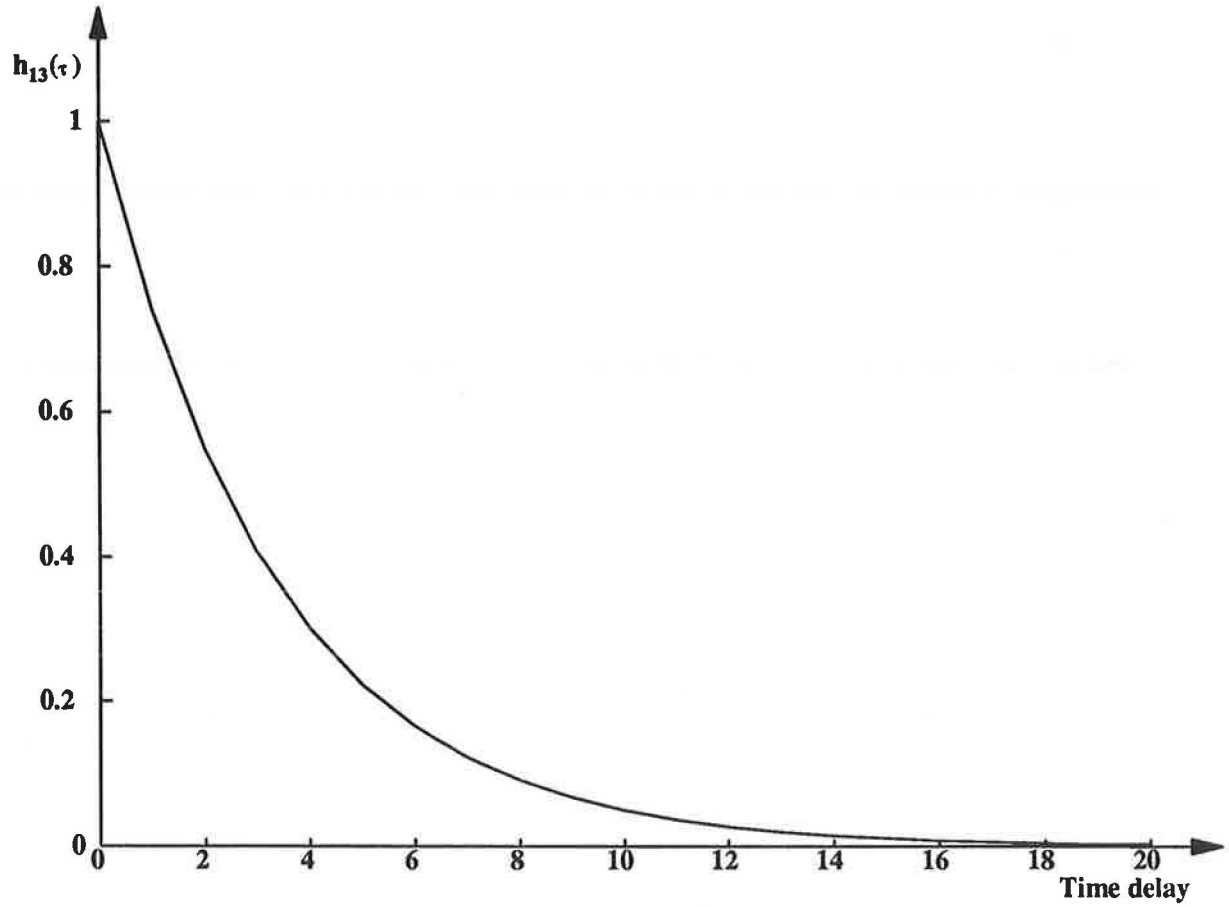

Figure 9 : The estimated linear response function for the third input channel

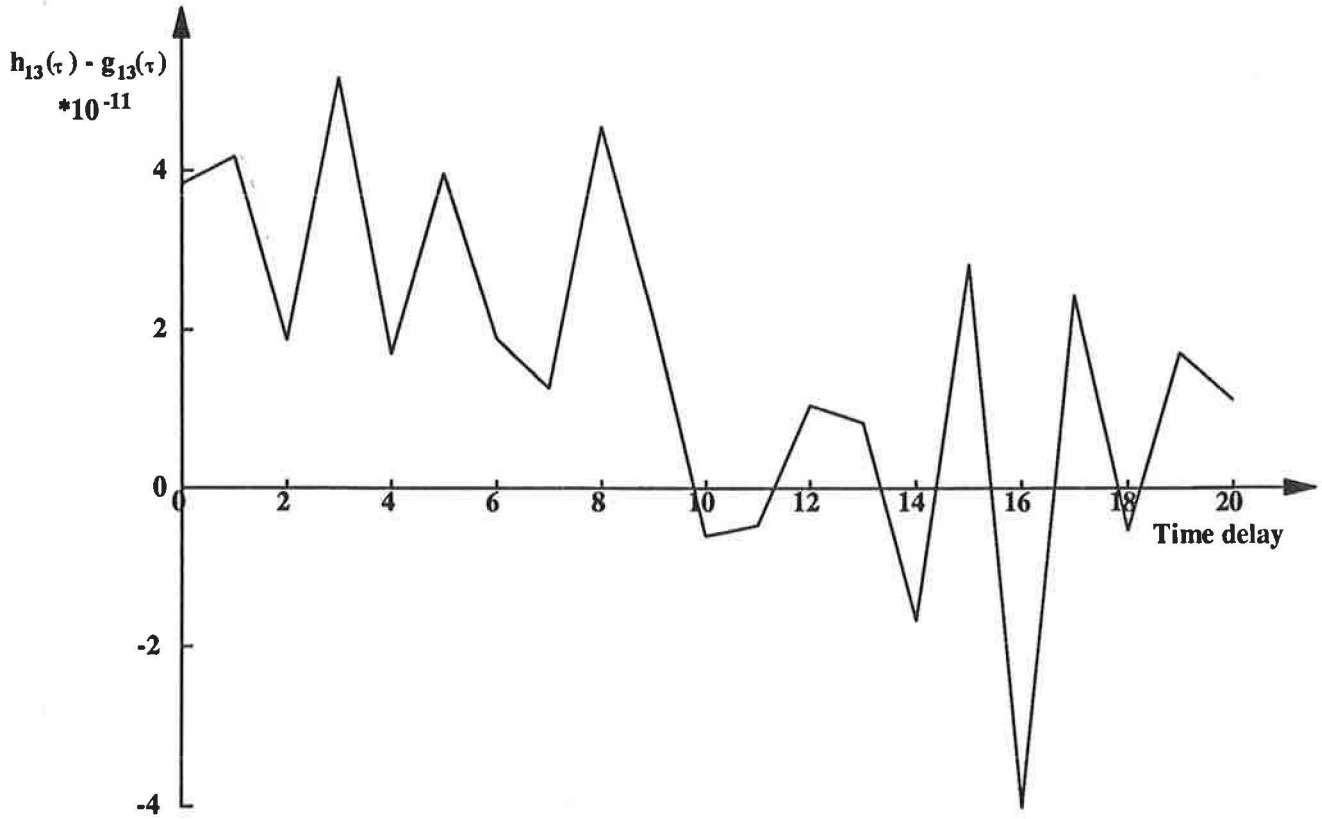

Figure 10 : The difference between the estimated and known linear response functions for the third input channel

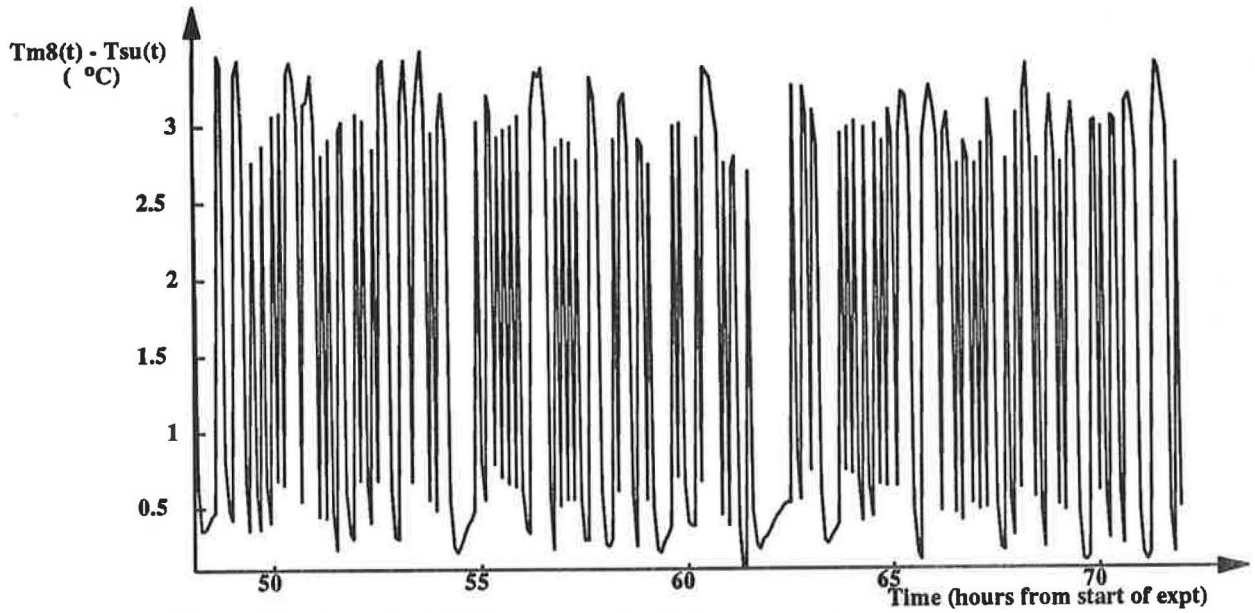

Figure 11 : A typical 24 hour sample of the temperature difference between the eighth Meyer ladder sensor and the surface of the ceiling

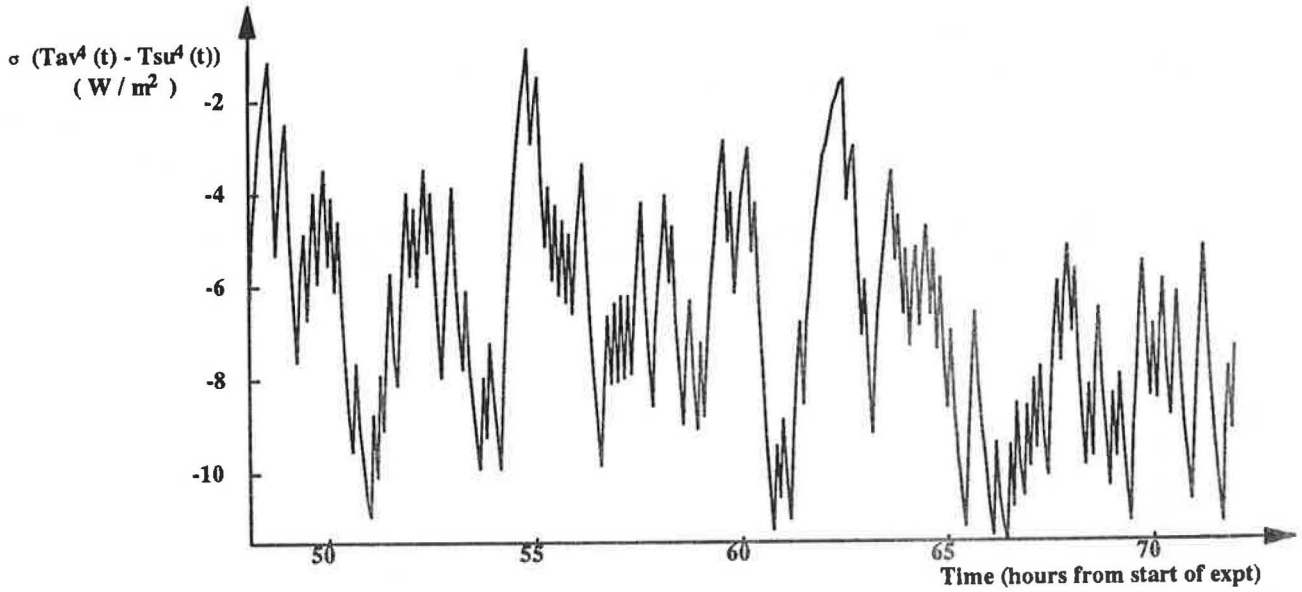

Figure 12 : A typical 24 hour sample of the difference between the fourth powers of the temperatures of the ceiling surface and average of the remaining surfaces

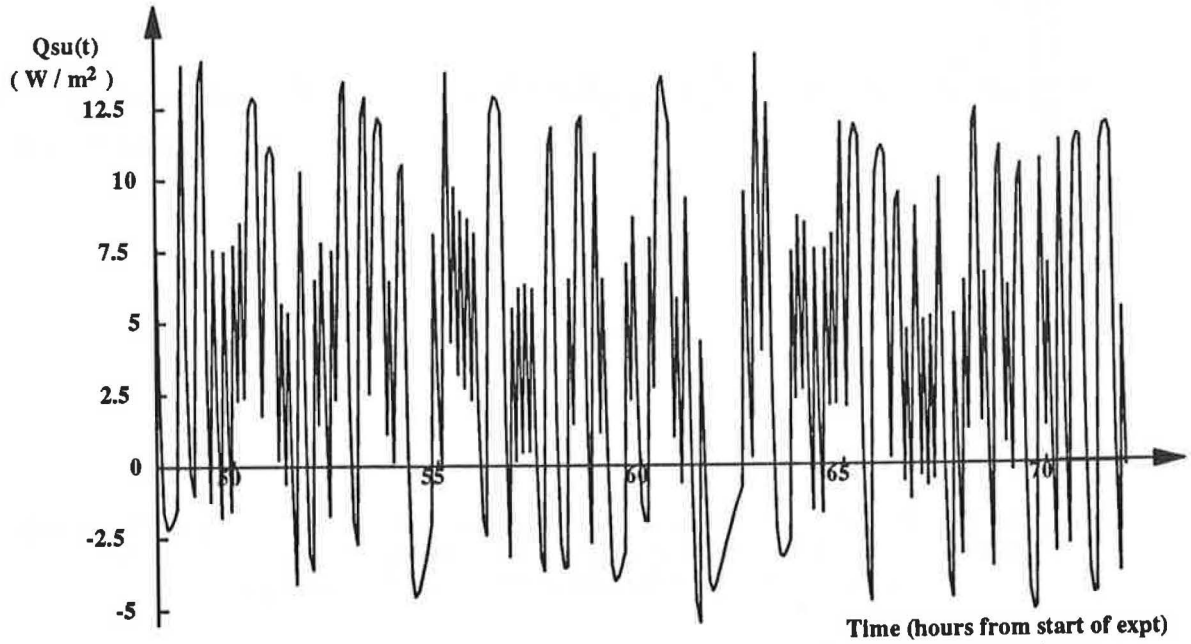

Figure 13 : A typical 24 hour sample of the heat flux at the ceiling surface

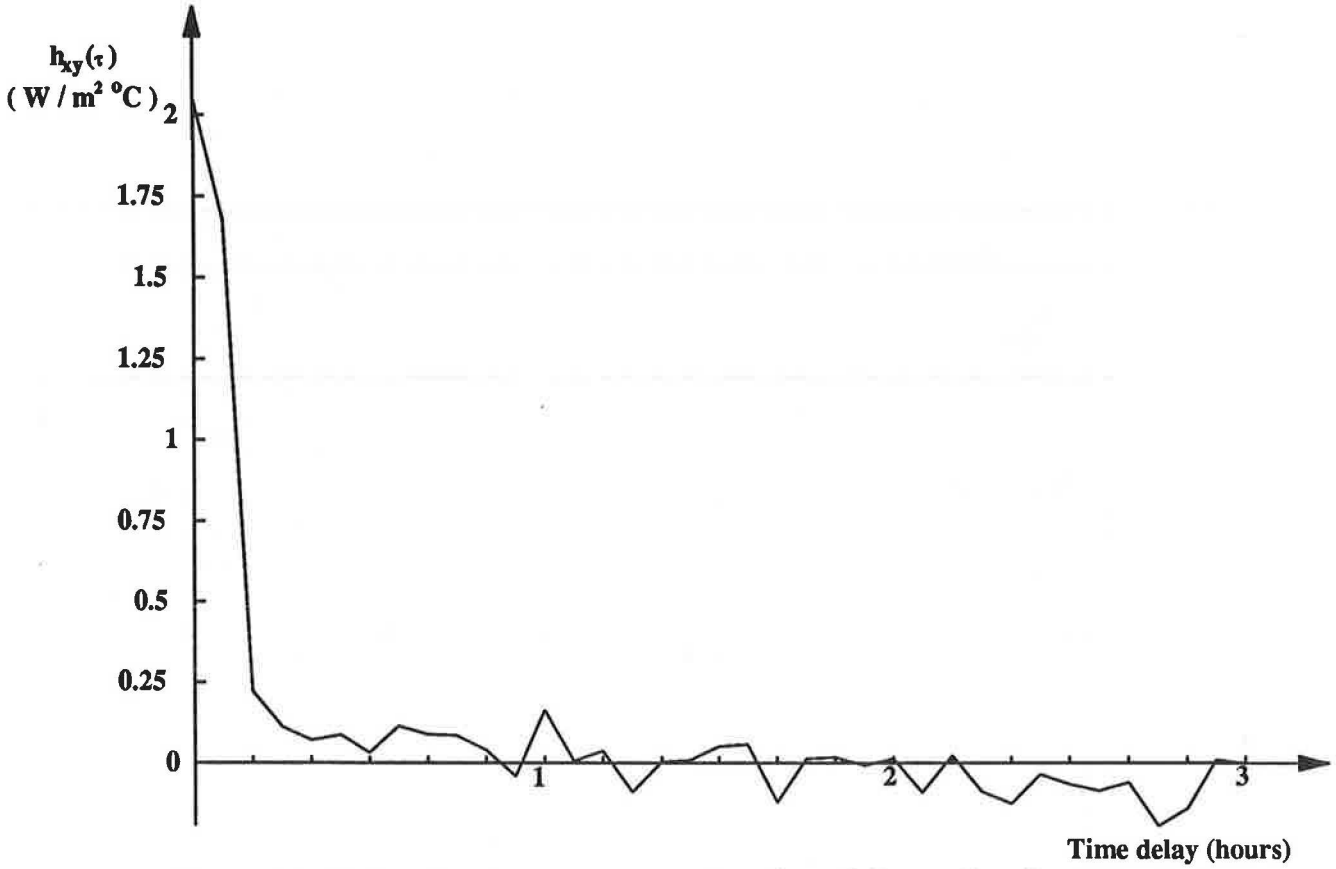

Figure 14 : Estimated linear response function of the surface heat flux to the temperature difference between the eighth ladder sensor and the ceiling surface (The response function of the convective process)

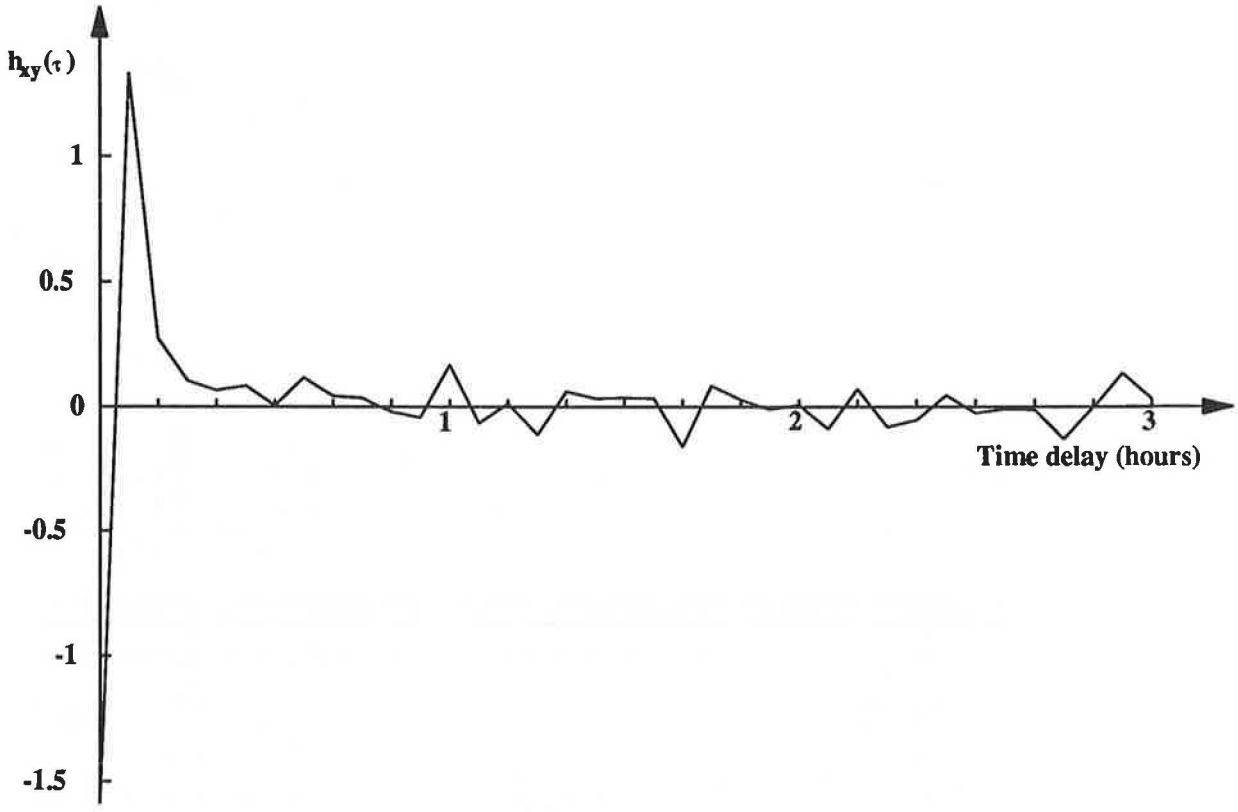

Figure 15 : Estimated linear response function of the surface heat flux to the difference between the fourth powers of the surface temperatures (The response function of the radiative process)

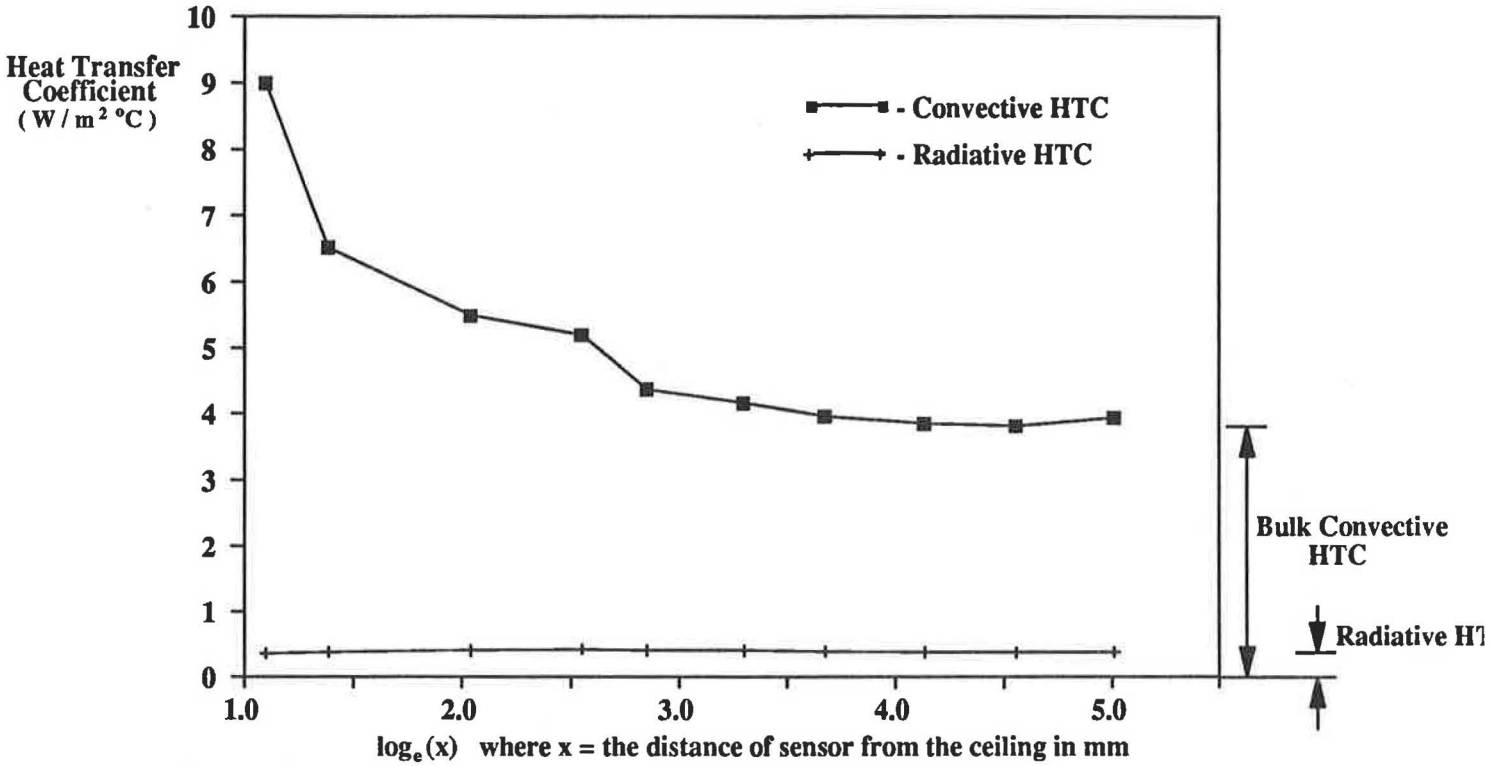

Figure 16 : Estimated convective and radiative heat transfer coefficienys for each Meyer ladder sensor position from the multi-input approach

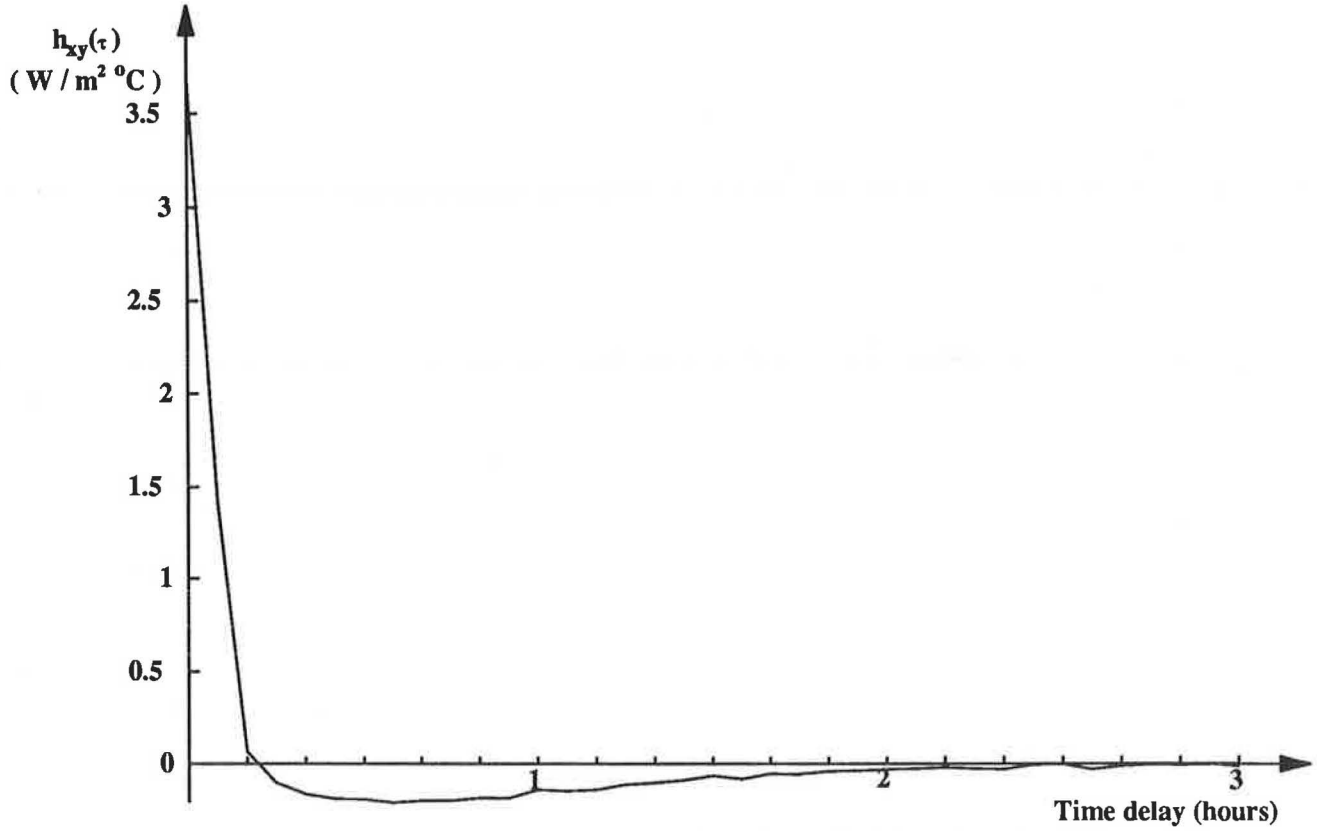

Figure 17 : Estimated linear response function of the surface heat flux to the temperature difference between the eighth ladder sensor and the ceiling using the single-input formalism

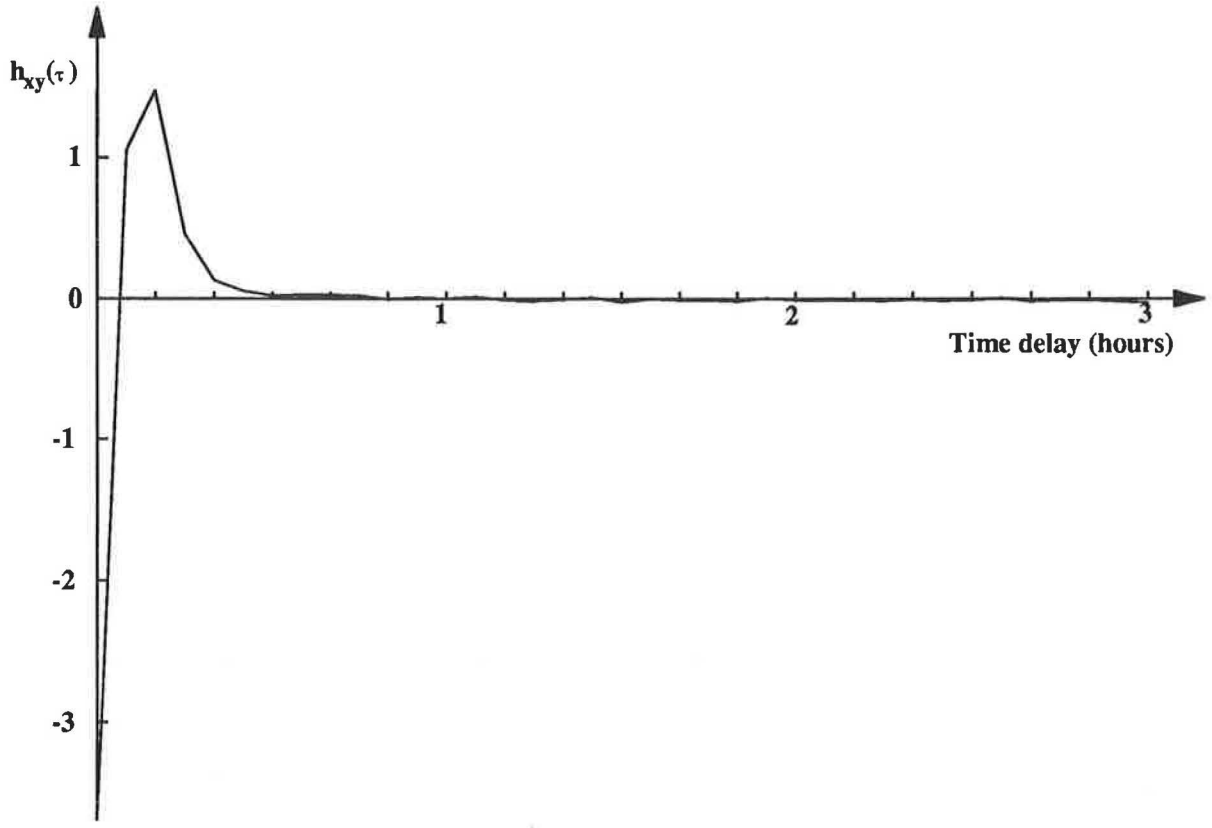

Figure 18 : Estimated linear response function of the surface heat flux to the difference between the fourth powers of the surface temperatures, using the single-input formalism

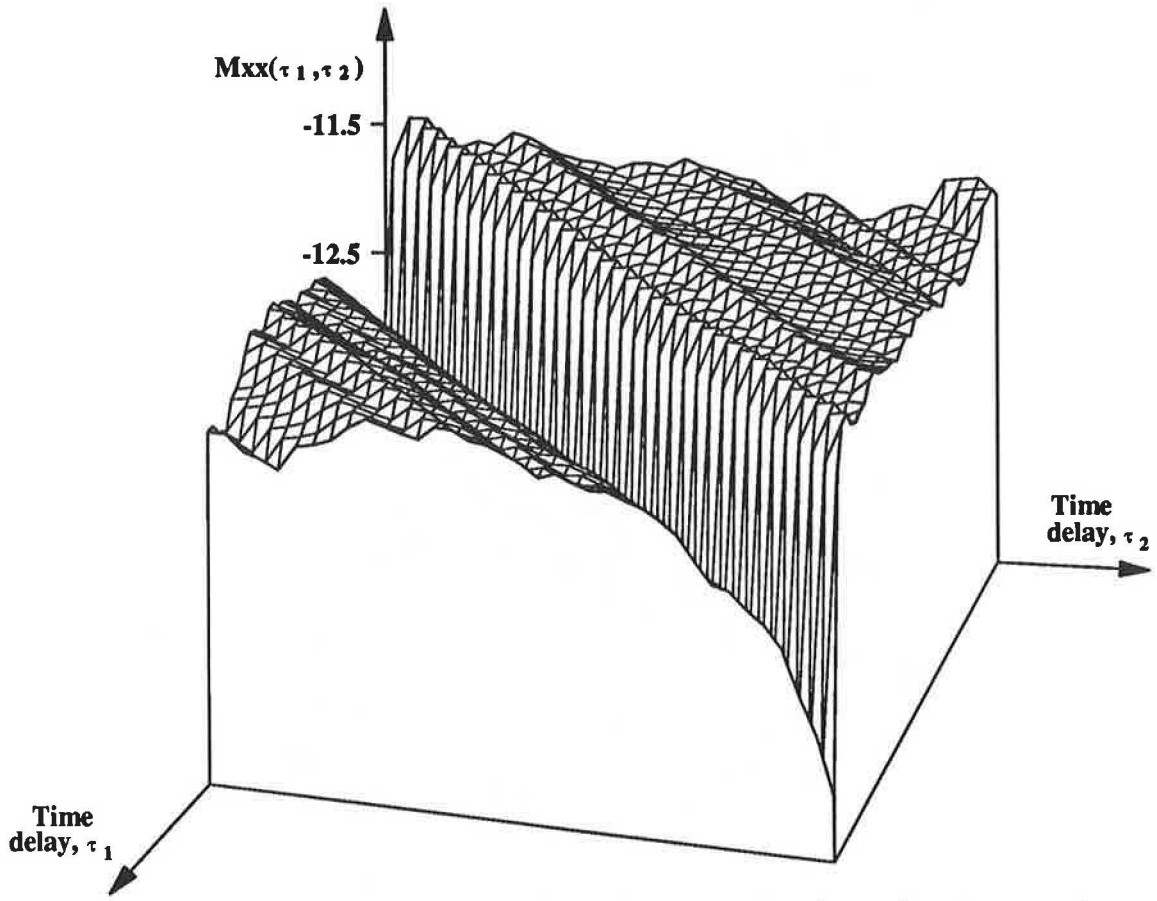

Figure 19 : Second order cross covariance between the air-surface temperature difference and the surface-surface temperature difference

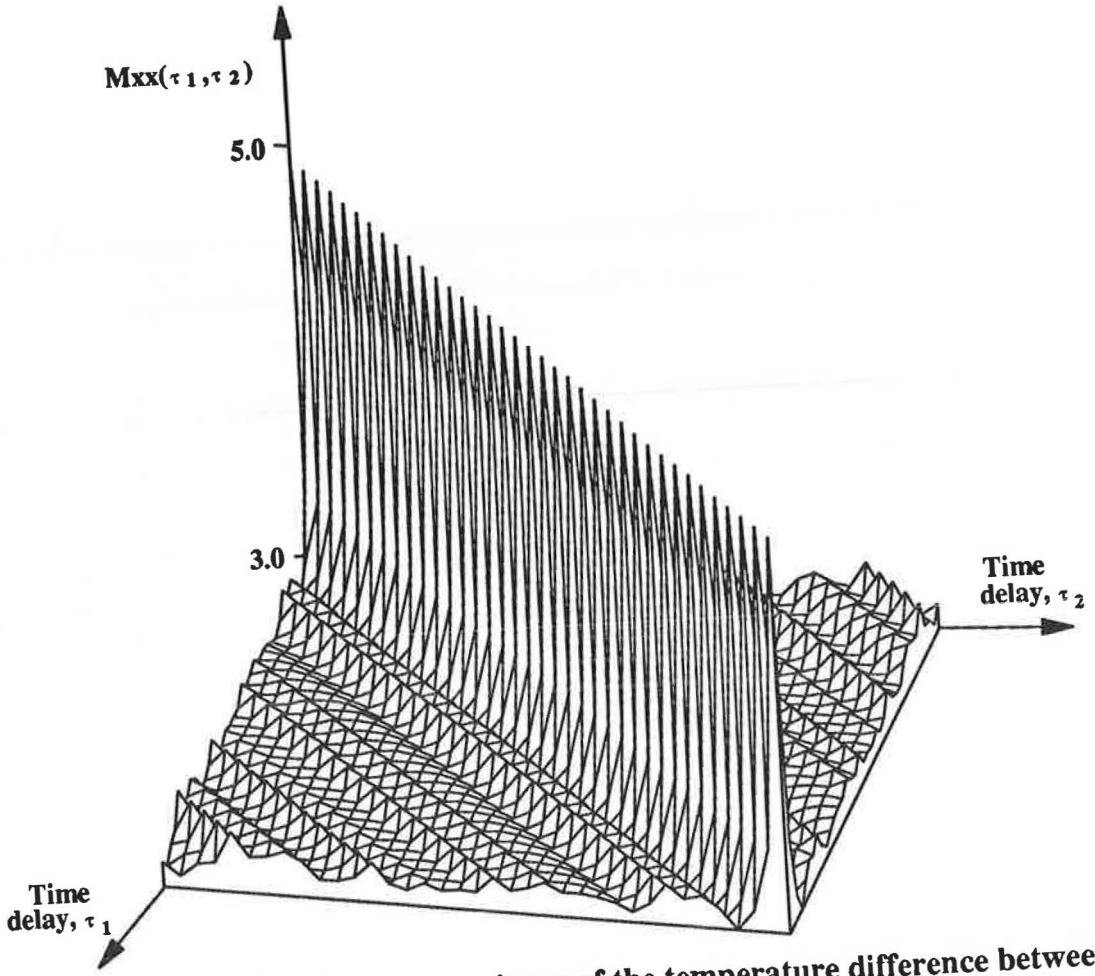

Figure 20 : Second order auto covariance of the temperature difference between the eighth Meyer ladder sensor and the surface of the ceiling

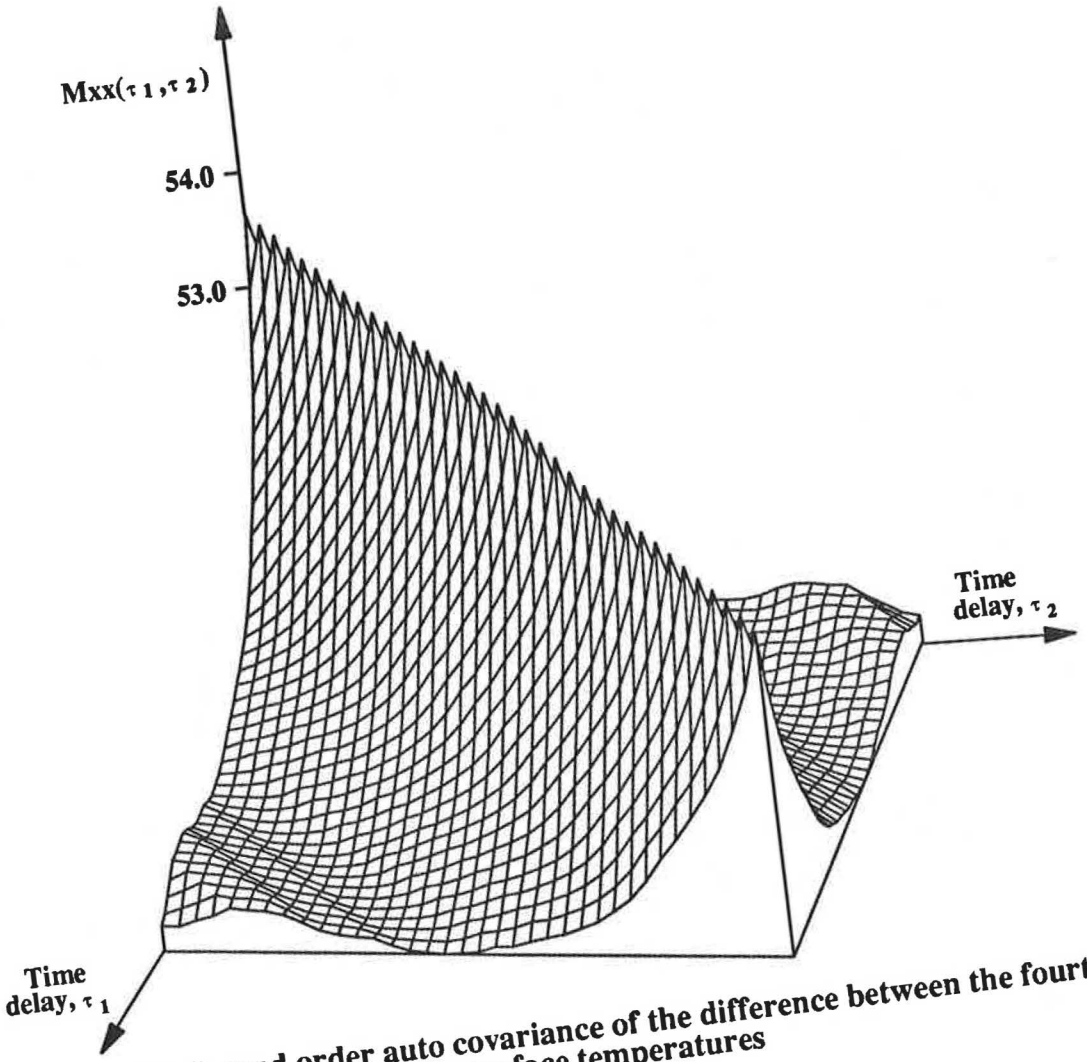

Figure 21 : Second order auto covariance of the difference between the fourth powers of the surface temperatures

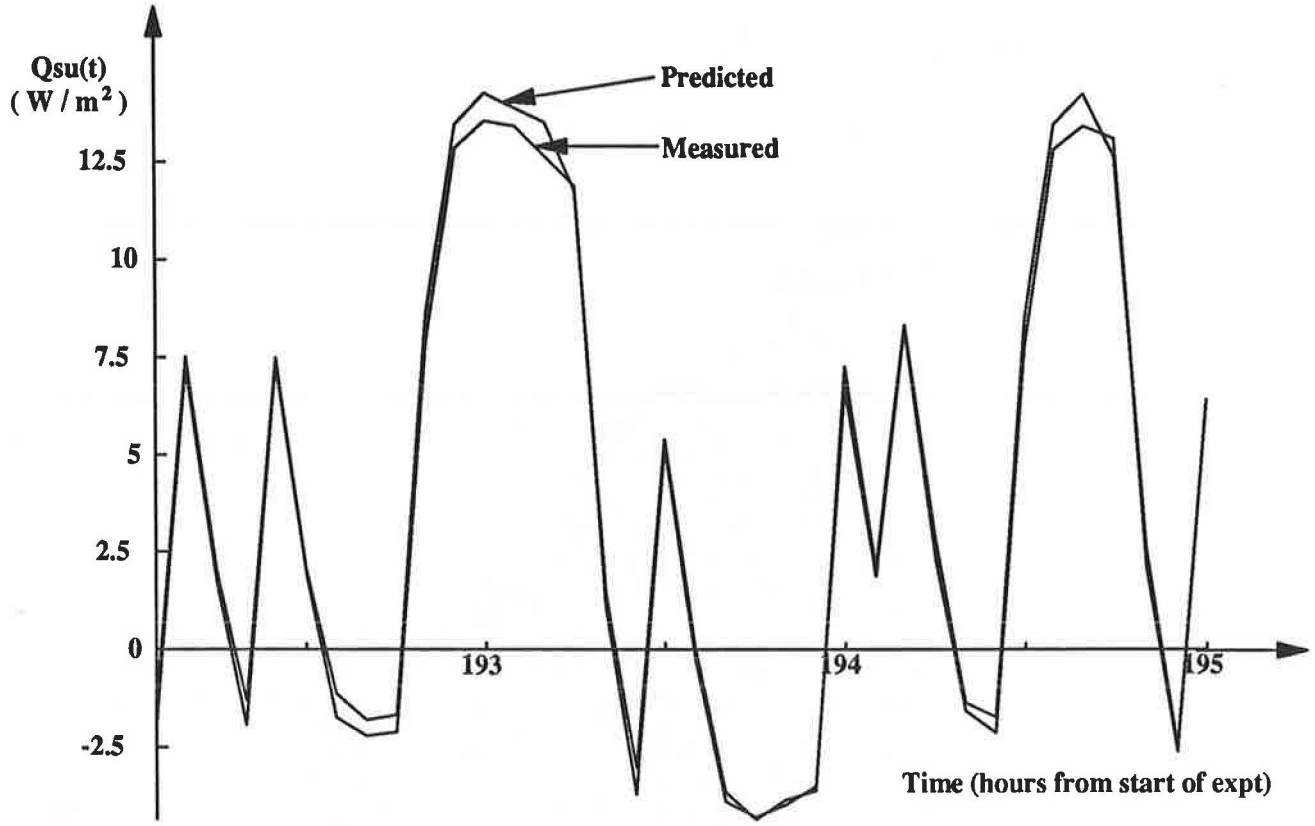

Figure 22 : A sample of the measured and predicted (using the convective and radiative response functions estimated by the multi-input formalism) heat flux at the surface of the ceiling

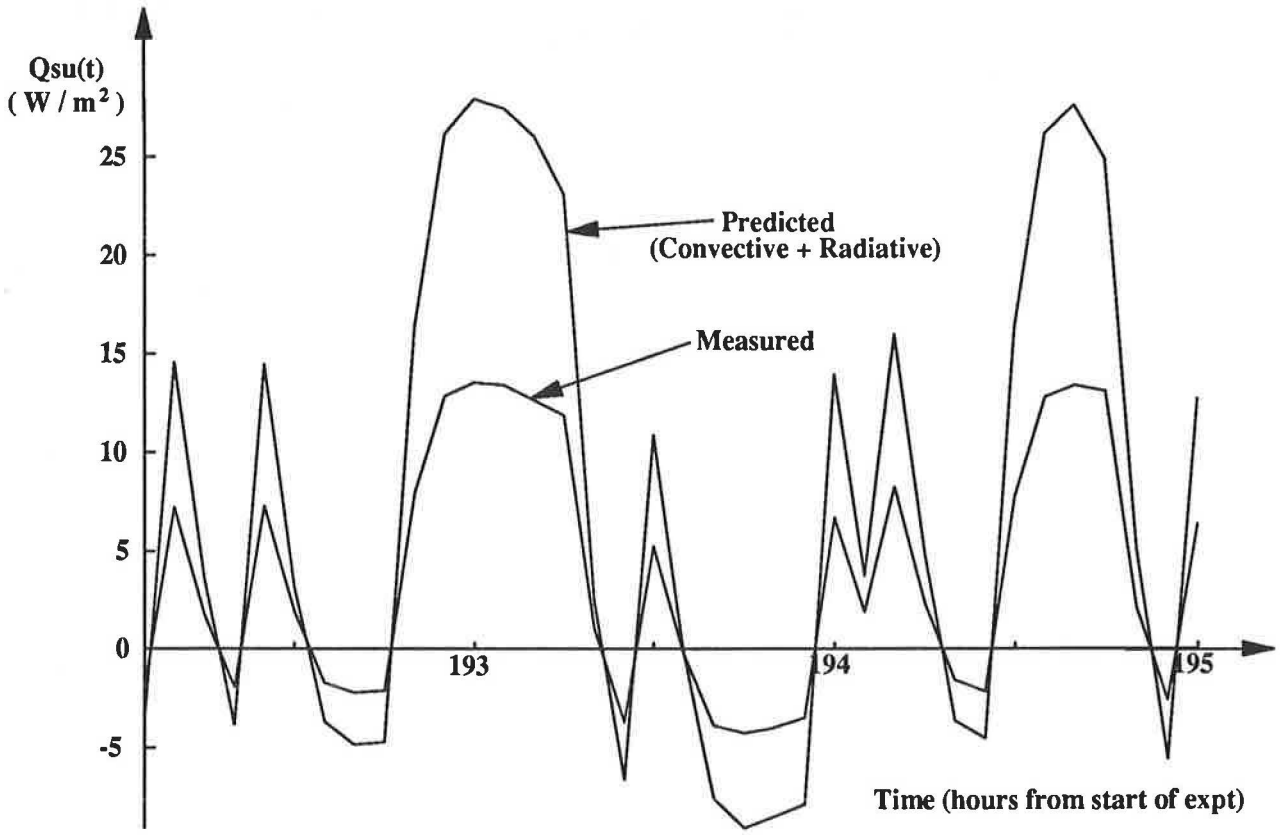

Figure 23 : A sample of the measured and predicted (using the convective and radiative response functions estimated by the single-input formalism) heat flux at the surface of the ceiling

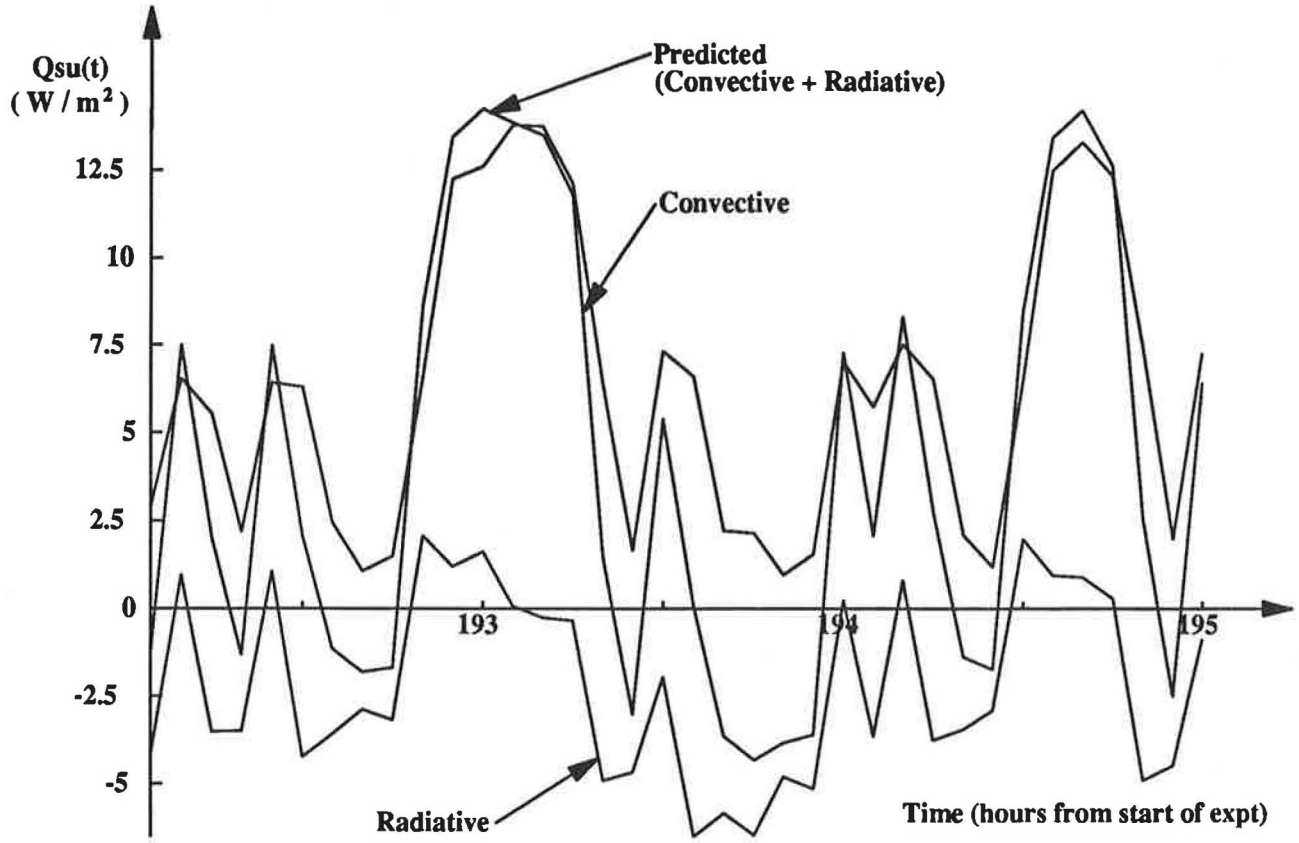

Figure 24 : A sample of the predicted heat flux at the ceiling surface, split into it's convective and radiative components, as predicted from the convective and radiative response functions estimated by the multi-input formalism